



1 **Evaluation on the effect of regional joint control measures in changing**
2 **photochemical transformation: A comprehensive study of the**
3 **optimization scenario analysis**

4 Li LI^{1,2#}, Shuhui ZHU^{2#}, Jingyu AN^{2#}, Min ZHOU², Hongli WANG^{2*}, Rusa YAN², Liping QIAO²,
5 Cheng Huang^{2*}, Xudong TIAN³, Lijuan SHEN⁴, Jeremy C AVISE⁵, Joshua S FU⁶

- 6 1. School of Environmental and Chemical Engineering, Shanghai University, Shanghai, 200444, China
7 2. State Environmental Protection Key Laboratory of the Cause and Prevention of Urban Air Pollution Complex,
8 Shanghai Academy of Environmental Sciences, Shanghai 200233, China
9 3. Zhejiang Environmental Monitoring Center, Hangzhou, 310014, China
10 4. Jiaxing Environmental Monitoring Station, Jiaxing, 314000, China
11 5. Laboratory for Atmospheric Research, Washington State University, Pullman, Washington, USA.
12 6. Department of Civil & Environmental Engineering, University of Tennessee, Knoxville, TN 37996, USA

13
14 *Correspondence to: C. Huang (huangc@saes.sh.cn) and H. L. WANG (wanghl@saes.sh.cn)

15 #These three people contribute equally.
16

17 **Abstract:** Heavy haze usually occurs in winter in eastern China. To control the severe air pollution
18 during the season, comprehensive regional joint-control strategies were implemented throughout a
19 campaign. To evaluate the effectiveness of these strategies and to provide some insight into
20 strengthening the joint-control mechanism, the influence of control measures on levels of air
21 pollution were estimated. To determine the influence of meteorological conditions, and the control
22 measures on the air quality, in a comprehensive study, the 2nd World Internet Conference was held
23 during December 16~18, 2015 in Jiaxing City, Zhejiang Province in the Yangtze River Delta (YRD)
24 region. We first analyzed the air quality changes during four meteorological regimes; and then
25 compared the air pollutant concentrations during days with stable meteorological conditions. Next,
26 we did modeling scenarios to quantify the effects caused due to the air pollution control measures.
27 We found that total emissions of SO₂, NO_x, PM_{2.5} and VOCs in Jiaxing were reduced by 56%, 58%,
28 64% and 80%, respectively; while total emission reductions of SO₂, NO_x, PM_{2.5} and VOCs over the
29 YRD region are estimated to be 10%, 9%, 10% and 11%, respectively. Modelling results suggest
30 that the regional controls (including Jiaxing and surrounding area) reduced PM_{2.5} levels in Jiaxing
31 between 5.5%-16.5% (9.9% on average), while local control measures contributed 4.5%-14.4%,
32 with an average of 8.8%. Our implemented optimization analysis compared with previous studies
33 also reveal that local emission reductions play a key role in air quality improvement, although it
34 shall be supplemented by regional linkage. In terms of regional joint control, to implement pollution
35 channel control 48 hours before the event is of most benefit in getting similar results. Therefore, it
36 is recommended that a synergistic emission reduction plan between adjacent areas with local
37 pollution emission reductions as the core part should be established and strengthened, and emission
38 reduction plans for different types of pollution through a stronger regional linkage should be



39 reserved.

40 **Keywords:** PM_{2.5}; regional joint control; meteorology; YRD

41 **1 Introduction**

42 High concentrations of PM_{2.5} has attracted much attention due to its impact on visibility (Pui
43 et al., 2014), human health (West et al., 2016) and global environment. To control air pollution
44 situation in China, the Ministry of Ecology and Environment of the People's Republic of China has
45 released a lot of policies, which can generally be divided into long-term action plans (such as the
46 Clean Air Action Plan (2013-2017), the Five-year Action Plans) and short-term control measures
47 (such as Clean Air Protection at Mega Events, Air Pollution Warning and Protection Measures).
48 China has successfully implemented some mega event air pollution control plans and ensured good
49 air quality, including the 2008 Beijing Olympics (Kelly and Zhu, 2016); the 2010 World Expo in
50 Shanghai (CAI-Asia, 2010); the 2010 Guangzhou Asian Games (Liu et al., 2013); the 2014 Asia-
51 Pacific Economic Cooperation Forum (APEC) (Liang et al., 2017); 2014 Summer Youth Olympics
52 in Nanjing (CAI-Asia, 2014) and the 2015 China Victory Day Parade (Victory Parade 2015) (Liang
53 et al., 2017), etc. After implementation of these control measures, it is important to understand how
54 effective these strategies are.

55 The 2nd World Internet Conference was held in Wuzhen, Jiaxing, Zhejiang during 16-18
56 December, 2015. To reduce air pollution during the conference, Zhejiang Province and the Regional
57 Air-pollution Joint Control Office of the Yangtze River Delta (YRD) region developed an Action
58 Plan for Air Pollution Control during the Conference (henceforth referred to as the Action Plan),
59 which clarified target goals, time periods for implementing controls, regions in which the controls
60 would be applied, and the control measures to be implemented, as described below. **Targets:**
61 achieve an Air Quality Index (AQI) below 100 in “key areas”, an AQI below 150 in “control areas”,
62 and to achieve significant improvement of the air quality in the surrounding (or buffer) regions
63 outside of the control areas. **Time Periods:** the time periods of interest for implementing various
64 controls include the early stage (3 months before the conference), the advanced stage (2 weeks to 4
65 days before the conference) and the central stage (3 days before and 2 days after the conference).
66 **Regions:** areas within a 50km radius, within a 100km radius and outside of a 100km radius from
67 the centre of Wuzhen were classified as key areas, control areas and buffer areas, respectively. These



68 areas cover 9 cities including Jiaxing, Huzhou, Hangzhou, Ningbo and Shaoxing in Zhejiang
69 province, Suzhou and Wuxi in Jiangsu province and Xuancheng in Anhui province.

70 Many studies have provided descriptive analysis of the changing concentrations of air
71 pollutants during mega events. Some have reported the emission reductions and related air quality
72 changes. However, different air pollution control targets, different control measures, and different
73 locations, may cause big different effects among those strategies. In this paper, the reduction in
74 $PM_{2.5}$ achieved through the Action Plan is investigated further to help quantify the level of $PM_{2.5}$
75 reduction that can be attributed to different aspects of the Action Plan. An integrated emission-
76 measurement-modelling method described in the next section including analysis of multi-pollutant
77 observations, backward trajectory and potential source contribution analyses, estimates of pollutant
78 emission reductions, and photochemical model simulations were adopted to conduct a
79 comprehensive assessment of the impact of control measures on air quality improvement based on
80 three aspects: meteorological conditions, pollutant emission reductions of local sources, and
81 regional contributions.

82 **2 Methodology**

83 In order to strengthen the regional air pollution joint-control mechanism in the YRD region,
84 various measures and their implementation were systematically reviewed, and the qualitative and
85 quantitative relationships between the implementation of measures, changes in emissions of air
86 pollution sources and air quality improvement were studied. Specifically, the impact of measures
87 such as management and control of coal-burning power plants, production restriction and
88 suspension of industrial enterprises, motor vehicle limitation and work site suspension, were
89 investigated. In addition, the role of meteorology (in particular, transport) was assessed in terms of
90 its influence on the relevance and effectiveness of various measures, and ways of optimising air
91 quality control measures and emergency emission reductions under heavy pollution during major
92 events were evaluated.

93 To assess the effectiveness of the various controls outlined in the Action Plan, emission
94 reductions associated with those controls were calculated, and photochemical modelling was
95 conducted to determine the change in $PM_{2.5}$ attributed to specific controls. On this basis, an
96 assessment of how to optimise control measures was carried out with respect to both the area in



97 which the emission reduction took place, as well as the start time for implementing the controls (i.e.,
98 how far in advance do the controls need to be implemented). Analysis of the numerical modelling
99 results is focused on the effectiveness of the control measures with respect to regional transport of
100 pollutants in the YRD region.

101 2.1 Measurements

102 The online observational station was set up at the Shanxi supersite of Zhejiang Province (30.82
103 N, 120.87 E), which was located at the core area for pollution-control measures. On-line hourly
104 PM_{2.5} mass concentration, carbonaceous aerosols, elements, and ionic species were measured by the
105 Synchronized Hybrid Ambient Real-time Particulate Monitor (SHARP, model 5030, Thermo Fisher
106 Scientific Corporation, USA), the OC/EC carbon aerosol analyzer (Model-4, Sunset Laboratory
107 Corporation, USA), the Xact multi-metals monitor (XactTM 625, PALL Corporation, USA), and
108 the Ambient Ion Monitor-Ion Chromatograph (AIM IC, model URG 9000, URG Corporation, USA),
109 respectively. Meteorological parameters, consisting of wind speed, wind direction, temperature,
110 pressure, and relative humidity, were measured as well.

111 PM_{2.5} concentration data conform to the standards of data quality control published by Ministry
112 of Ecology and Environment of the People's Republic of China.

113 A semi-continuous Sunset OC/EC analyser was used to measure OC and EC mass loadings at
114 the observation site by adopting NIOSH-5040 protocol based on thermal-optical transmittance
115 (TOT). The ambient air was first sampled into a PM_{2.5} cyclone inlet with a flow rate of 8 L·min⁻¹.
116 The OC and EC were collected on a quartz fiber filter with an effective collection area of 1.13 cm².
117 The analyzer was programmed to collect aerosol for 45 min at the start of each hour, followed by
118 the analysis of carbonaceous species during the remainder of the hour. The analysis procedure is
119 described in detail by Huang et al. (2018)

120 The ionic concentrations of nitrate, sulphate, chloride, sodium, ammonium, potassium, calcium
121 and magnesium (Na⁺, K⁺, Ca²⁺, NH₄⁺, Mg²⁺, NO₃⁻, SO₄²⁻, Cl⁻) in the fine fraction (PM_{2.5}) were
122 measured with a 1-hour time resolution using the AIM IC. The sample analysis unit is composed by
123 an anion and a cation ion chromatographs (Dionex ICS-1100), which was using guard columns with
124 potassium hydroxide eluent (KOH) for the anion system and methane sulfonic acid (MSA) eluent
125 for the cation system. The limit of the detection reported by the manufacturer is 0.1 ug/m³ for all



126 species. The operation principle of AIM-IC is described in detail by Markovic et al. (2012)

127 Hourly ambient mass concentrations of sixteen elements (K, Ca, V, Mn, Fe, As, Se, Cd, Au,
128 Pb, Cr, Ni, Cu, Zn, Ag, Ba) in PM_{2.5} were determined by the Xact multi-metals monitor. In brief,
129 the Xact instrument samples the air through a section of filter tape at a flow rate of 16.7 lpm using
130 a PM_{2.5} sharp cut cyclone. The exposed filter tape spot then advances into an analysis area where
131 the collected PM_{2.5} is analyzed by energy-dispersive X-ray fluorescence (XRF) to determine metal
132 mass concentrations. The sequence of sampling and analysis were performed continuously and
133 simultaneously on an hourly basis.

134 2.2 Potential Source Contribution Analysis

135 TrajStat is a HYSPLIT model developed by Chinese Academy of Meteorological Sciences and
136 NOAA Air Resources Laboratory based on geographic information system (GIS). It uses statistical
137 methods to analyze air mass back trajectories to cluster trajectories and compute potential source
138 contribution function (PSCF) with observation data and meteorological data included (Wang et al.,
139 2009).

140 PSCF analysis is a conditional probability function using air mass trajectories to locate
141 pollution sources. It can be calculated for each 1° longitude by 1° latitude cell by dividing the
142 number of trajectory endpoints that correspond to samples with factor scores or pollutant
143 concentrations greater than specified values by the number of total endpoints in the cell (Zeng et al.,
144 1989). Therefore, pollution source areas are indicated by high PSCF values. Since the deviation of
145 PSCF results could increase with the raise of distance between cell and receptor, therefore a weight
146 factor (W_{ij}) was adopted in this study to lower the uncertainty of PSCF results. PSCF and W_{ij}
147 calculations are described in Eq. (1) and Eq. (2), where m_{ij} is the number of trajectory endpoints
148 greater than specified values in cell (i, j), n_{ij} is the number of total endpoints in this cell (Zeng et al.,
149 1989; Polissar et al., 1999).

$$150 \quad P = \frac{m_{ij}}{n_{ij}} \cdot W(n_{ij}) \quad (1)$$

$$151 \quad W(n_{ij}) = \begin{cases} 1.00, & 80 < n_{ij} \\ 0.70, & 20 < n_{ij} \leq 80 \\ 0.42, & 10 < n_{ij} \leq 20 \\ 0.05, & n_{ij} \leq 10 \end{cases} \quad (2)$$

152 In this study, the TrajStat modelling system was used to analyze potential source contribution



153 areas of PM_{2.5} in Jiaxing during different pollution episodes with the combination of GDAS
154 meteorological data provided by the NCEP (National Center for Environmental Prediction).
155 Pollution trajectories corresponded to those trajectories with PM_{2.5} hourly concentration higher
156 than 75 µg/m³.

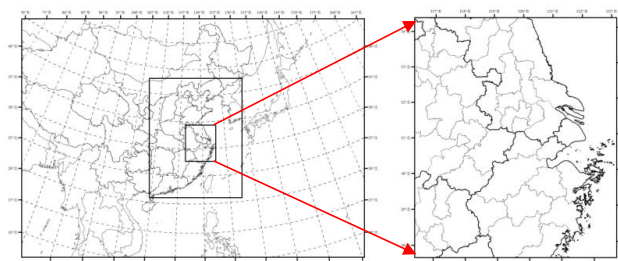
157 **2.3 Model setup for separating meteorological influence and control measures**

158 **2.3.1 Model selection and parameter settings**

159 In this study, the WRF-CMAQ/CAMx air quality numerical modelling system was used to
160 evaluate the improvement in air quality resulting from the control measures outlined in the Action
161 Plan. It takes into account of modeling variations from different air quality models. For the
162 mesoscale meteorological field, we adopted the WRF model Version 3.4
163 (<https://www.mmm.ucar.edu/wrf-model-general>), the CAMx model Version 6.1
164 (<http://www.camx.com/>) and the CMAQ model Version 5.0 (Nolte et al., 2015;
165 <http://www.cmascenter.org/cmaq/>). The chemical mechanism utilized in CMAQ was the CB05 gas
166 phase chemical mechanism (Yarwood, et al., 2005) and AERO5 aerosol mechanism, which includes
167 the inorganic aerosol thermodynamic model ISORROPIA (Nenes, et al., 1998) and updated SOA
168 yield parameterizations. The gaseous and aerosol modules used in CAMx are the CB05 chemical
169 mechanism and CF module, respectively. The aqueous-phase chemistry for both models is based on
170 the updated mechanism of the Regional Acid Deposition Model (RADM) (Chang et al., 1987).
171 Particulate Source Apportionment Technology (PSAT) coupled in the CAMx is applied to quantify
172 the regional contributions to PM_{2.5} as well. The WRF meteorological modeling domain consists of
173 three nested Lambert projection grids of 36km-12km-4km, with 3 grids larger than the
174 CMAQ/CAMx modeling domain at each boundary. WRF was run simultaneously for the three
175 nested domains with two-way feedback between the parent and the nest grids. Both the three
176 domains utilized 27 vertical sigma layers with the top layer at 100hpa, and the major physics options
177 for each domain listed in Table 1. For the CMAQ/CAMx modelling domain shown in Figure 1, we
178 adopted a 36-12-4km nested domain structure with 14 vertical layers, which were derived from the
179 WRF 27 layers. The two outer domains cover much of eastern Asia and eastern China, respectively,
180 while the innermost domain covers the YRD region. The simulation period was from 1-18
181 December, 2015, during which 1-7 December was utilized for model spin-up and 8-18 December



182 was the key period for analysis of the modelling results with control measures.



183
184 Fig 1. Modeling domain

185 Table 1 Parameterization scheme of the physical processes in the WRF model

Physical Processes	Parameterization Scheme	Reference
Microphysical Process	Purdue Lin Scheme	(Lin, 1983)
Cumulus Convective Scheme	Grell-3 Scheme	(Grell and Dévényi, 2002)
Road Process Scheme	Noah Scheme	(Ek, 2003)
Boundary Layer Scheme	Yonsei University (YSU) Scheme	(Hong, 2006)
Long-wave Radiation	RRTM Long-wave Radiation Scheme	(Mlawer et al., 1997)
Short-wave Radiation Scheme	Goddard Short-wave Radiation Scheme	(Chou and Suarez, 1999)

186 Initial and boundary conditions (IC/BCs) for the WRF modeling were based on 1-degree by 1-
187 degree grids FNL Operational Global Analysis data that are archived at the Global Data
188 Assimilation System (GDAS). Boundary conditions to WRF were updated at 6-hour intervals for
189 D01.

190 Anthropogenic source emission inventory in YRD is based on a most recent inventory
191 developed by our group (Huang et al., 2011; Li et al., 2011; Liu et al., 2018). The emission inventory
192 for areas outside YRD in China is derived from the MEIC model (Multi-resolution Emission
193 Inventory of China, latest data for 2012 (<http://www.meicmodel.org>) and anthropogenic emissions
194 over other Asian region are from the MIX emission inventory for 2010 (Li et al., 2017). Biogenic
195 emissions are calculated by the MEGAN v2.1 (Guenther et al., 2012). The Sparse Matrix Operator
196 Kernel Emissions (SMOKE, <https://www.cmascenter.org/smoke>) model is applied to process these
197 emissions for modeling inputs that is more detailed emission processes and not usually used in China.

198 2.3.2 Model performance

199 Prior to evaluating the effectiveness of the control measures and reactions, the performance of

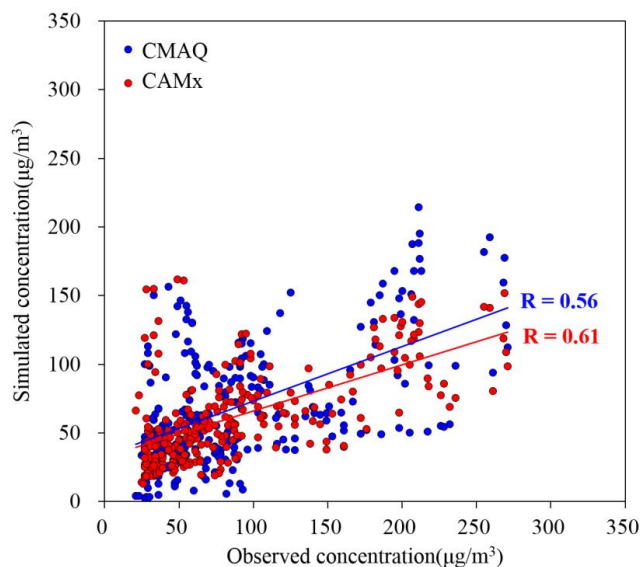


200 the modelling system was evaluated to ensure it was able to reasonably reproduce the observed
201 meteorological conditions and PM_{2.5} levels. Statistical indexes used for model evaluation include
202 Normalised Mean Bias (NMB), Normalised Mean Error (NME) and Index of Agreement (I).

203 Observational data from the Shanxi supersite in Jiaxing City were compared with model results
204 for model evaluation verification. Table 2 shows the summary statistics for the main meteorological
205 parameters simulated with the WRF model and hourly PM_{2.5} concentrations simulated by CMAQ.
206 Among the meteorological parameters, wind speed is slightly over predicted with the IOA value of
207 28%, while temperature, relative humidity and pressure all have NMB values greater than 0.9.
208 Figure 2 compares the simulated and observed PM_{2.5} concentrations at the Shanxi supersite. In
209 general, model predicted data are lower than the observed data with the NMB value of -22% to -
210 30%, the NME value of 45% to 47% and the I value of 0.67 to 0.70 (Table 2). Overall, these statistics
211 for both the meteorological parameters and simulated PM_{2.5} are generally consistent with the results
212 in other published modelling studies (Zheng et al., 2015; Wang et al., 2014; Zhang et al., 2011; Fu et
213 al., 2016; Li et al., 2015b; Li et al., 2015a), which suggests that the simulation performance is
214 acceptable.

215 Table 2 Statistics of simulation verification for meteorological parameters and hourly PM_{2.5} concentration

Statistical indexes	Wind speed	Temperature	Relative humidity	Air pressure	CAMx-PM _{2.5}	CMAQ-PM _{2.5}
NMB	28%	3%	-9%	0%	-30%	-22%
NME	33%	14%	12%	0%	45%	47%
IOA	0.81	0.97	0.93	1.00	0.67	0.70

216
217Fig. 2 Scatter plot of the simulated and observed PM_{2.5} at the Shanxi supersite

2.3.3 Method for quantifying the effectiveness of a control

219 Quantifying the PM_{2.5} reduction in response to emission reductions was done using the so
220 called Brute Force Method (BFM) (Burr and Zhang, 2011), where a baseline scenario was simulated
221 using unadjusted emissions (i.e., those emissions that would have occurred in absence of the Action
222 Plan) and a campaign scenario was modelled based on the emission controls outlined in the Action
223 Plan. In both cases, the same meteorology and chemical boundary conditions were utilized to drive
224 the photochemical model simulations. Through a comparative analysis of the scenarios, a relative
225 improvement factor (RF) for a given atmospheric pollutant, resulting from emission controls, can
226 be calculated and combined with ground based observations to assess the improvement in air quality
227 associated with those emission controls.

$$228 \quad RF = (C_b - C_s) / C_b \quad (3)$$

$$229 \quad C_d = C_o \cdot RF \quad (4)$$

230 where C_b is the simulated pollutant concentration in the baseline scenario ($\mu\text{g}/\text{m}^3$), C_s is the
231 pollutant concentration in the campaign scenario ($\mu\text{g}/\text{m}^3$), C_o denotes the actual observed
232 concentration at the site ($\mu\text{g}/\text{m}^3$) and C_d is the concentration improvement caused by the control
233 measures ($\mu\text{g}/\text{m}^3$). Utilizing models in a relative sense to assess the efficacy of emission controls on
234 air quality is common practice in regulatory modelling, with the assumption that there may be biases
235 in the absolute concentrations simulated by a modelling system, but that the relative response of that



236 system will reflect the response observed in the atmosphere (US EPA, 2014).

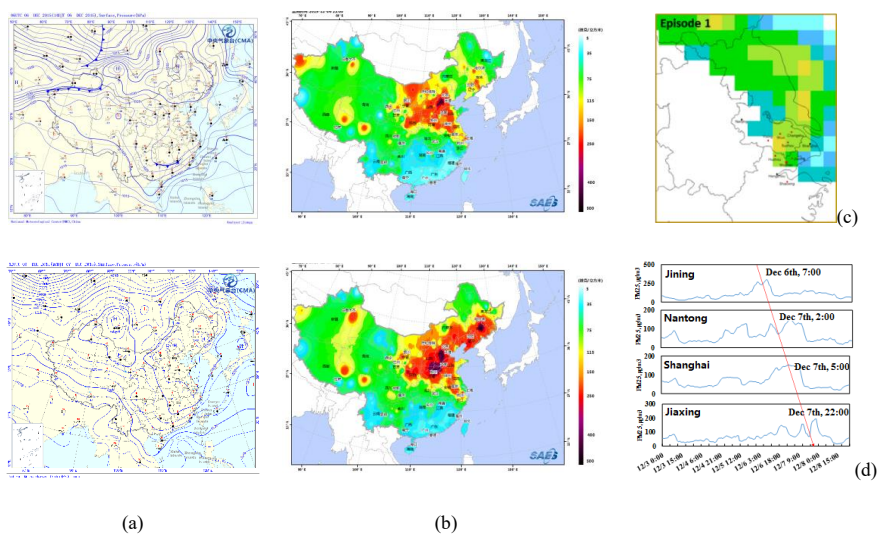
237 **3 Results and discussion**

238 **3.1 Photochemical transformation changes of air pollutants during the campaign**

239 Ground observation data show that from December 1 to December 23, Jiaxing City
240 experienced four distinct physical and chemical processes that contributed to the observed pollution
241 levels at different times. For each of these processes, this study has comprehensively in the
242 integrated emission-measurement-modeling method considered the backward air flow trajectory,
243 potential contribution source areas, meteorological conditions and the variation of PM_{2.5}
244 concentration to analyse the evolution of the observed air quality.

245 **3.1.1 Pollution process before the campaign with local emission accumulation as the main** 246 **contributor**

247 The first time period of interest was from December 6 to December 8. Analysis about the
248 potential source contribution areas resulting from PSCF modelling suggests that the polluted air
249 mass primarily originated from the northwest and northerly airstreams, passing Shandong, the
250 eastern coastal areas of Jiangsu and Shanghai and into northern Zhejiang, as is shown in Fig. 3.
251 Analysis of the large-scale weather patterns showed that pollution occurred in Beijing, Tianjin,
252 Shandong peninsula and northern Jiangsu as a result of cold air with polluted air mass transported
253 into the region on the morning of December 5. In the southern part of Shandong province, the PM_{2.5}
254 concentration peak appeared on the morning of December 6, while the PM_{2.5} concentration peak
255 appeared around midnight on December 7 at the coastal area of Jiangsu. On December 6, the
256 development of warm and humid air flow, resulted in increasing ground humidity, which
257 contributed to the growth of secondary fine particles and the gradual accumulation of pollution in
258 northern Zhejiang and the surrounding areas of Shanghai. On December 7, affected by the surface
259 high-pressure system, the spread of pollution was slow, and the spatial extent of the pollution in
260 northern Zhejiang expanded. Therefore, during this time period, the pollution was primarily affected
261 by regional transport and worsened by stagnant local conditions in Jiaxing.

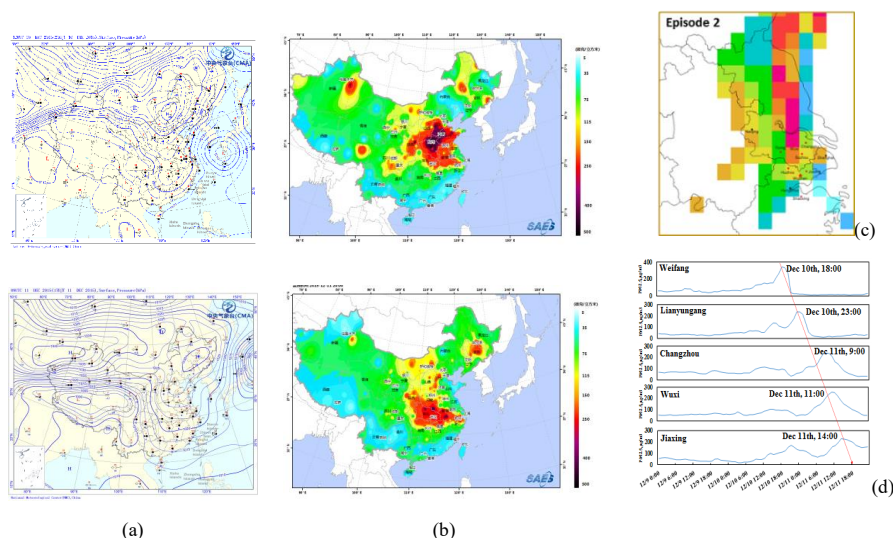


262 Fig. 3 Analysis of (a) the large-scale weather patterns, (b) distribution of PM_{2.5} concentrations, (c) potential regional
263 sources, (d) PM_{2.5} time series for selected sites during December 6 to December 8, 2015



264 3.1.2 Pollution process during the campaign with the southward motion of the weak cold air

265 The second time period of interest was from December 10 to December 11. Analysis about potential source
266 contribution areas suggests that the polluted air mass mainly came from northern regions, passing from south-eastern
267 Shandong peninsula and central-eastern Jiangsu to northern Zhejiang. From the large-scale weather pattern, the
268 diffusion of weak cold air on December 10 gradually transported the pollution in the upper reaches of the region to
269 the YRD region. The pollution peaked in areas such as Lianyungang in northern Jiangsu on the evening of December
270 10. On December 11, the PM_{2.5} concentration peak appeared in central and southern Jiangsu as a result of northern
271 weak air flow. The pollution was further transported into Zhejiang province with the expansion in influenced areas
272 as is shown in Figure 5. Therefore, the pollution process was mainly affected by the transportation of polluted air
273 mass caused by the southward motion of cold air.



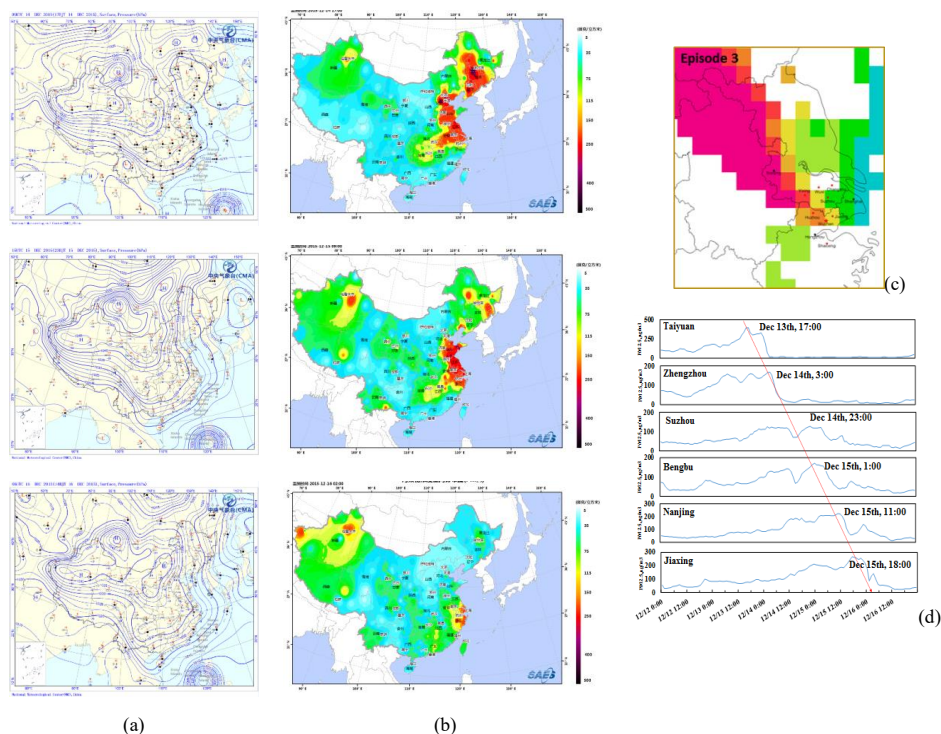
274 Fig. 4 Analysis of (a) the large-scale weather patterns, (b) distribution of PM_{2.5} concentrations, (c) potential regional sources, (d)
275 PM_{2.5} time series for select sites during December 10 to December 11, 2015

276 3.1.2 Heavy pollution process during the campaign with the transit and transportation of strong cold air

277 The third period of interest was from December 13 to the early hours of December 16. Analysis of the potential
278 source contribution areas suggest that the polluted air mass mainly came from the northwest direction, passing
279 through south-eastern Shanxi, western Shandong, eastern Anhui and western Jiangsu to Zhejiang province. On
280 December 14, affected by the cold air transportation in the north, northern pollution hit Hebei, Henan and Anhui
281 provinces, with the highest degree of pollution on the 14th. On December 15, the further spread of cold air caused
282 the transport of pollution into Jiangsu and Zhejiang. The northern part of Zhejiang province was in the centre of
283 pollution on the 15th, which worsened the pollution and expanded the scope of pollution, as is shown in Figure 3-
284 12. On December 16, under the control of the high-pressure system in northern Zhejiang, the air mass gradually



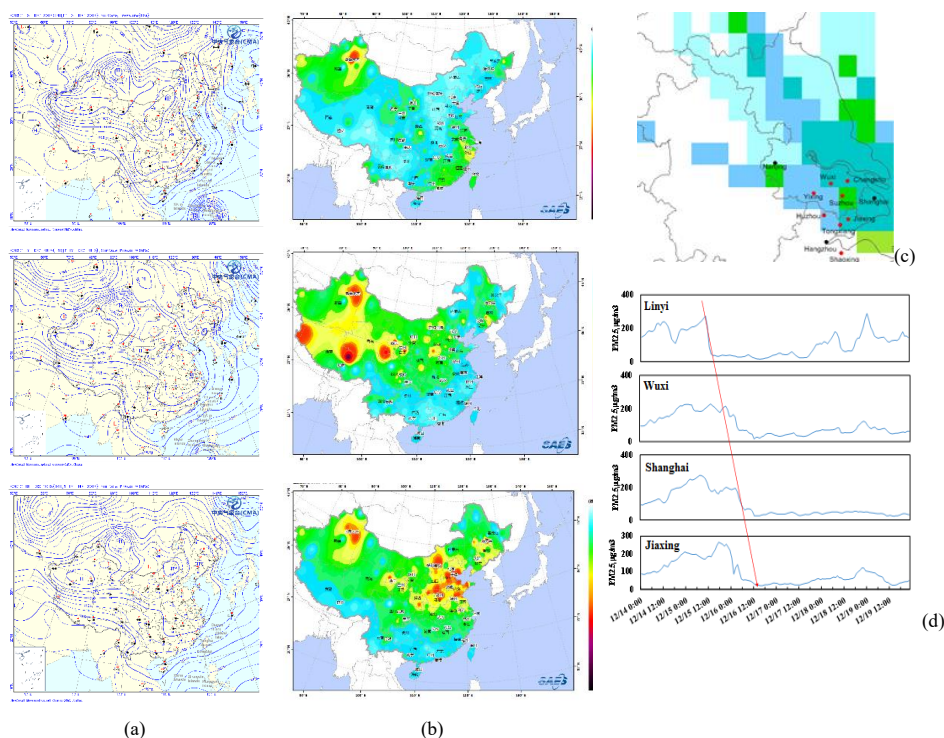
285 moved eastward and the air quality improved in the morning. Therefore, for this time period, large-scale
286 transportation was the main factor leading to the increase in pollutant levels.



287
288 Fig. 5 Analysis of (a) the large-scale weather patterns, (b) distribution of PM_{2.5} concentrations, (c) potential regional sources, (d)
289 PM_{2.5} time series for select sites during December 14 to December 16, 2015

290 3.1.3 Pollution removal process caused by clean cold air during the conference

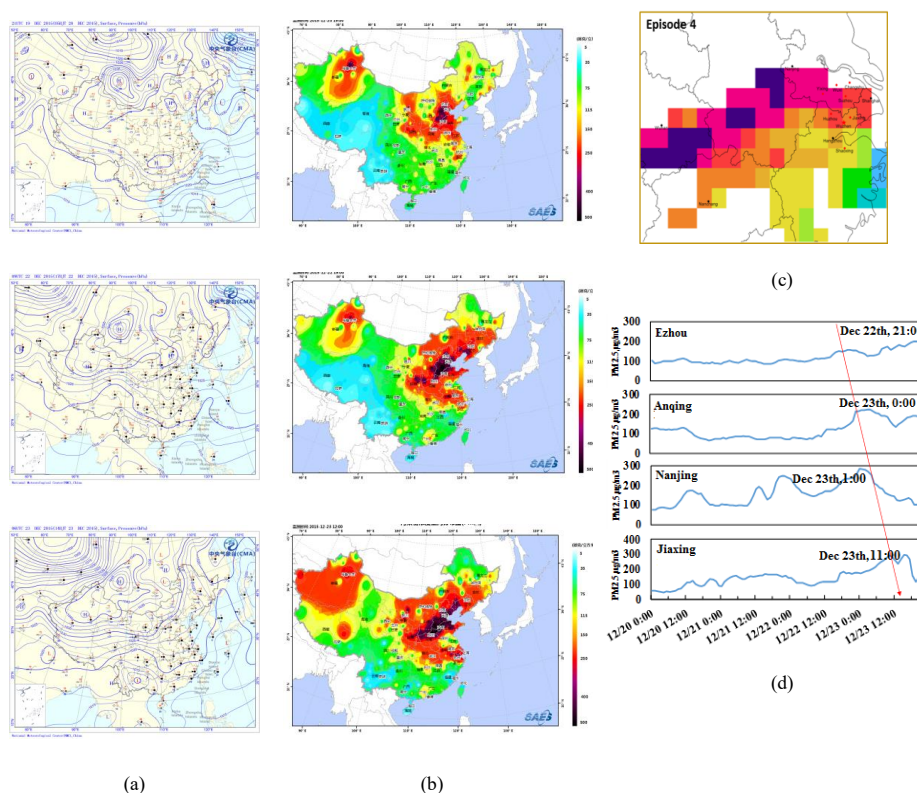
291 During the conference from December 16 to December 18, weather was affected by the large-scale southward
292 transport of cold dry air in northern Zhejiang, resulting in lower temperature and relative humidity, as well as a
293 significant improvement in the air quality. On the 17th and the 18th, under the control of a high pressure system in
294 northern Zhejiang, the sea level pressure increased, the humidity was lower and the wind speed was reduced.
295 Because of the emission reduction effect of the control measures, the pollutant accumulation rate was likely slowed
296 and the air quality in northern Zhejiang was good overall. From the analysis of potential sources, PM_{2.5}
297 concentrations in Shandong, Jiangsu and Shanghai were significantly reduced. The PM_{2.5} concentration during the
298 conference was mainly controlled by local emissions, as is shown in Figure 6.



299 Fig. 6 Analysis of (a) the large-scale weather patterns, (b) distribution of PM_{2.5} concentrations, (c) potential regional sources, (d)
300 PM_{2.5} time series for select sites during December 16 to December 18, 2015

301 3.1.4 Pollution process after the campaign with local emission accumulation as the main contributor

302 The fourth period of interest was from December 20 to December 23. Analysis of the potential source
303 contribution areas suggest that the polluted air mass mainly came from the southwest direction, passing through
304 southern Hubei, southern Anhui and south-western Jiangsu to northern Zhejiang. On December 20, controlled by a
305 stagnant air mass, Zhejiang province has a relatively low near-surface wind speed and little dispersion, resulting in
306 the accumulation of local pollutants. On December 21, northern Zhejiang was located in the centre of a high pressure
307 system with conditions conducive to little mixing, and therefore pollution occurred in some areas in northern
308 Zhejiang. On December 22, affected by the warm and humid southwest air flow, Zhejiang had experienced some
309 precipitation but the pollution in northern Zhejiang was not improved due to deep polluted air masses. In Hubei and
310 Anhui located in the southwest of Jiaxing City, high pollution levels appeared from the evening of December 22 to
311 the early hours of December 23 as is shown in Figure 7. On December 23, the further expansion of polluted air
312 masses resulted in serious pollution in Jiangsu and northern Zhejiang. In general, under these heavily polluted
313 conditions, the local accumulation of pollutants was mainly caused by stagnant conditions with little dispersion and
314 transport within southwest air stream.



315 Fig. 7 Analysis of (a) the large-scale weather patterns, (b) distribution of PM_{2.5} concentrations, (c) potential regional sources, (d)
316 PM_{2.5} time series for select sites during December 20 to December 23

317 3.2 Air quality changes under the same meteorological conditions before and after the campaign

318 3.2.1 Air quality changes under static meteorological conditions before and during the campaign

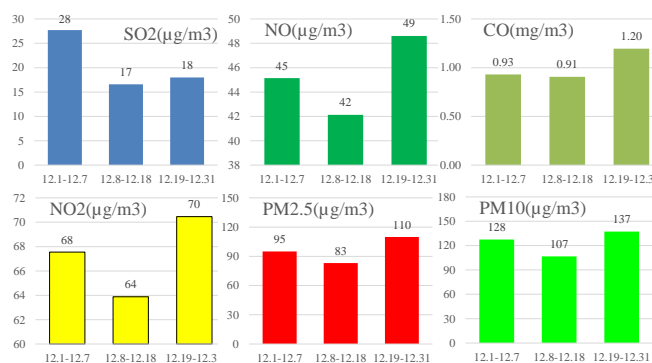
319 During the air pollution control campaign for the conference, air quality in Jiaxing City fluctuated greatly due
320 to the frequent southward motion of cold air from the north. Under static weather conditions, sources of atmospheric
321 pollution mainly came from the accumulation of pollution from local sources and sources in neighbouring areas.
322 Therefore, in order to eliminate the influence of the transportation process of the air mass, this study compared the
323 air quality status before, during and after the campaign in Jiaxing City under stagnant weather conditions (wind
324 speed less than 1m/s) and assessed the impact of control measures on ambient air quality in Jiaxing based on air
325 quality observation data.

326 Figure 8 shows the concentration levels of normal pollutants including SO₂, NO, CO, NO₂ and PM_{2.5} in Jiaxing
327 City before (December 1-7), during (December 8-19) and after the campaign (December 19-31) under stagnant
328 weather conditions. It can be seen that pollutant concentrations during the campaign were less than those before the
329 campaign, in which SO₂ had the most significant decline of 40.1%, NO_x, CO, PM_{2.5} and PM₁₀ declined 8.0%, 2.6%,
330 12.5% and 16.3%, respectively, indicating that control measures have significantly improved the air quality in



331 Jiaxing City, especially with respect to SO₂ and PM₁₀.

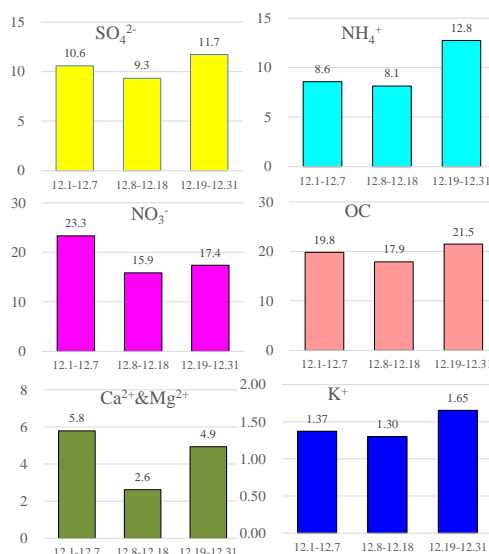
332 After the campaign, all the pollutant concentrations rebounded sharply. SO₂, NO, NO₂, CO, PM_{2.5}, PM₁₀
333 increased 8.3%, 15.4%, 10.3%, 31.8%, 32.2% and 28.6%, respectively. Concentrations of some pollutants were
334 even higher than those before the campaign, which suggests that the emission intensity of the sources had
335 significantly increased after the campaign.



336
337
338

Fig. 8 Comparison between air pollutant concentrations at Shanxi station before, during, and after the campaign under stagnant meteorological conditions

339 There are also some differences in concentrations of major chemical components of PM_{2.5} in Jiaxing City
340 before (December 1-7), during (December 8-19) and after the campaign (December 19-31) under stagnant weather
341 conditions, as shown in Figure 9. The concentrations of major chemical components of PM_{2.5} during the campaign
342 were less than those before the campaign, which is consistent with the conclusion about changes in normal pollutant
343 concentrations. On average, SO₄²⁻, NH₄⁺, NO₃⁻, OC mineral soluble irons (Ca²⁺ and Mg²⁺) and K⁺ declined 11.8%,
344 5.1%, 32.1%, 9.8%, 56.8% and 5.1%, respectively. Comparisons between the distribution of PM_{2.5} chemical
345 components before and during the campaign suggest that Ca²⁺ and Mg²⁺ decreased most significantly during the
346 control period, which indicates that the suspension of construction operations which result in dust emissions and
347 the rising frequency of rinsing and cleaning paved roads, significantly reduced dust emissions. During the campaign,
348 NO₃⁻ significantly decreased, indicating that vehicle control measures successfully reduced NO_x emissions and
349 subsequently the formation of inorganic aerosols. The significant decrease in SO₄²⁻ also shows that restricting and/or
350 suspending the operation of coal-burning power plants and industries in local and neighbouring cities played a very
351 positive role.



352
 353
 354

Fig. 9 Comparison between PM_{2.5} chemical components at Shanxi station before and after the campaign under static meteorological conditions

3.2.2 Air quality changes under the same air mass trajectory before and during the campaign

356 In order to distinguish the impact of meteorological conditions on air quality in Jiaying City and better analyse
 357 the effects of control measures on air quality during the conference, this study has combined meteorological
 358 conditions with backward air flow trajectory analysis and carried out a comparative study by selecting a relatively
 359 similar pollution period before and during the campaign. The first period occurred before the campaign from 12:00
 360 December 2 to 20:00 December 4, while the second period occurred during the campaign from 9:00 December 16
 361 to 5:00 December 18. Both of these periods were relatively unaffected by long-range transport of pollution into the
 362 study area, and have similar backward airflow trajectories and meteorological conditions. Table 3 and Figure 10
 363 compare average mass concentrations of pollutants (SO₂, NO_x, PM_{2.5} and PM₁₀) during these two periods. As can
 364 be seen from the figure, SO₂, PM_{2.5} and PM₁₀ decreased during the campaign by roughly 46%, 13% and 27%,
 365 respectively, while NO_x exhibited only a small decrease. This shows that without the impact of long-range transport,
 366 emission reduction measures carried out by local and surrounding cities play a significant role in defining the air
 367 quality in Jiaying.

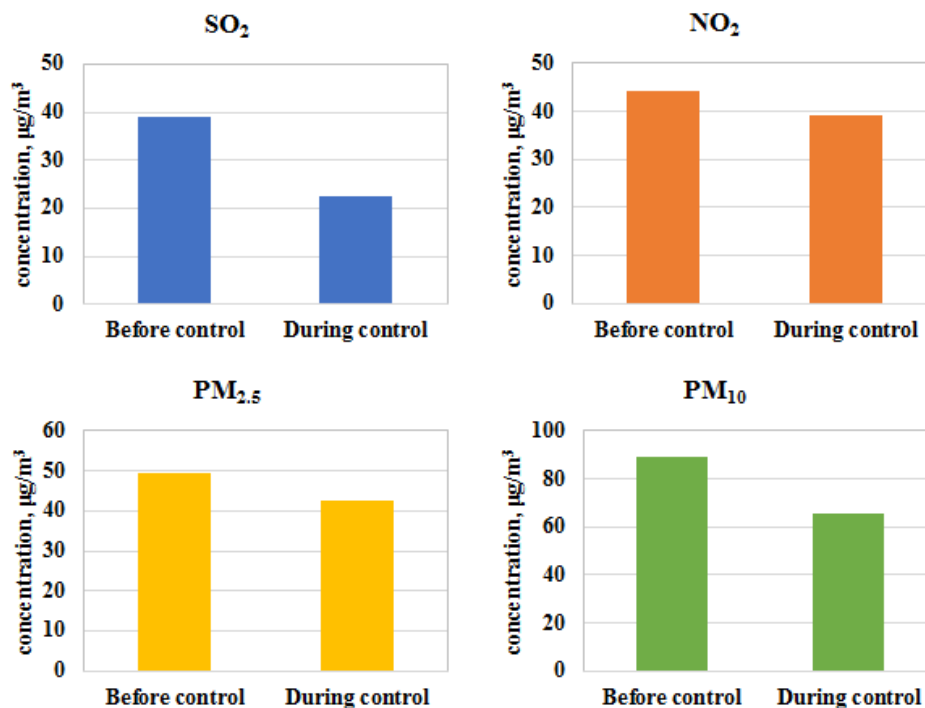
368
 369

Table 3 Concentrations of major pollutants under similar meteorological conditions before and during the campaign

Period	Time	Wind speed m/s	Wind direction °	Relative humidity %	Temperature °C	Pressure hPa	Visibility km	SO ₂ µg/m ³	NO ₂ µg/m ³	PM ₁₀ µg/m ³	PM _{2.5} µg/m ³
Before the	12.2 12:00-	3.1	268.0	59.2	8.2	102.6	22.8	39.1	44.4	89.5	49.4



campaign	12.4 20:00											
During the campaign	12.16 9:00-12.18 5:00	3.4	247.5	53.0	2.6	103.2	32.1	22.4	39.3	65.3	42.8	



370
 371
 372
 373

Fig. 10 Comparison between concentrations of major air pollutants in Jiaxing before and after the campaign under same meteorological conditions

374
 375
 376
 377
 378
 379

There were two regional pollution episodes that occurred during the campaign. The first was on December 10-12 caused by the southward motion of northern weak cold air. Polluted air masses from south-eastern Shandong peninsula passed through central eastern Jiangsu and into northern Zhejiang, affecting the air quality in Jiaxing. During this period, the average daily PM_{2.5} concentration in Jiaxing was 145.7 µg/m³, higher than the regional average, and its major chemical components were nitrate (31%), sulphate (18%) ammonium (13%) and organic carbon (13%), with obvious regional secondary pollution characteristics.

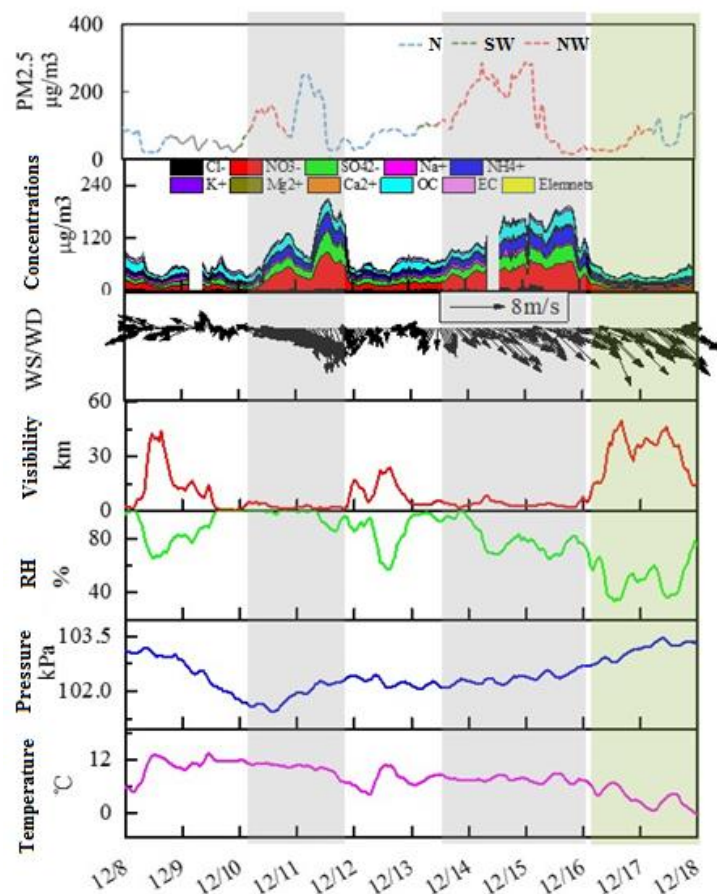


Fig.11 Changes in air quality and meteorological parameters in Jiaxing City during the campaign

380
381

382 The second episode occurred from December 14-15, and was caused by the transit of northwesterly strong cold
383 air. Polluted air masses came from the northwest direction, moved rapidly to the southeast, passed through Shanxi,
384 Hebei, west Shandong, east Anhui and west Jiangsu and ultimately into Zhejiang province. The air masses left
385 China through south-eastern Zhejiang on the early morning of the 16th. The YRD region was strongly affected by
386 the transport of the polluted air mass, with heavy pollution appearing and lasting for about one day over the YRD
387 region from north to south. PM_{2.5} peaked in Jiaxing on the 15th with a daily average of 201.6 µg/m³. The main
388 chemical components of PM_{2.5} during the episode were nitrate (25%), sulphate (14%), ammonium (12%) and
389 organic carbon (13%), which is consistent with an aged air mass as well as regional secondary pollution
390 characteristics.

391 The regional linkage was initiated from December 16 to December 18, combined with favourable mixing
392 conditions brought by the cold front. The overall air quality in the YRD region during this time period was good,
393 with an average daily PM_{2.5} concentration in Jiaxing of 45 µg/m³. The major chemical components during this

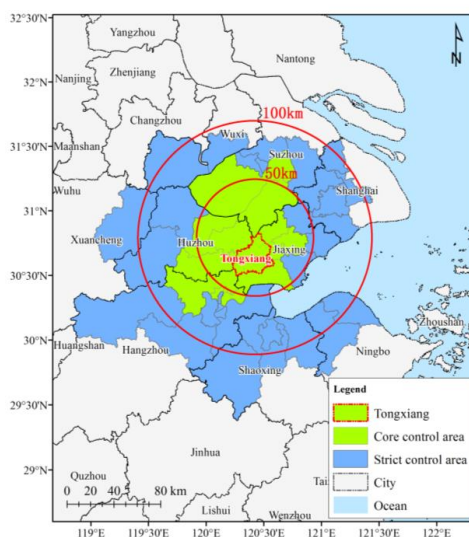


394 cleaner period were organic carbon (26%), nitrate (16%), ammonium (12%) and sulphate (9%), with some newly
395 formed particles and no obvious regional pollution characteristics, suggesting that air pollutants were mainly derived
396 from local emissions.

397 3.3 Emission reductions during the campaign

398 3.3.1 Control Measures adopted to reduce air pollutant emissions

399 The air quality assurance campaign for the 2nd World Internet Conference was from December 8 to December
400 18. In order to ensure the air quality during the conference, three provinces and Shanghai municipality in the YRD
401 region carried out joint control measures and established key areas, strict control areas, control areas and extension
402 areas, respectively, according to the degree of pollution impact from each region on the air quality in Jiaxing. Among
403 them, key areas and strict control areas included Zhejiang province (including Hangzhou, Ningbo, Huzhou, Jiaxing
404 and Shaoxing), Shanghai (including Jinshan and Fengxian), Jiangsu province (including Suzhou and Wuxi) and
405 Anhui province (including Xuancheng, Ma'anshan and Wuhu), as shown in figure 12.



406
407

Fig.12 Controlled regions in the Action Plan for Air Quality Control during the World Internet Conference

408 The following measures were taken in key areas and control areas: (1) Strictly control emissions from coal-
409 burning power plants: reduce emissions from power plants which have not completed ultra-low emission
410 transmission processes by 50% in key areas and by 30% in control areas. (2) Reduce emissions from key enterprises:
411 production restriction or suspension would be imposed on industries including cement, steel, construction materials,
412 petrochemicals, chemicals, casting, leather, non-ferrous metals, plate glass, pharmaceuticals, surface spraying and
413 printing. All key enterprises in key areas were discontinued (maximum production limits will be imposed on steel
414 and petrochemical industries), while key enterprises in control areas cut emissions by 30%. Enterprises which could



415 not meet the emission standards in a stable way, do not have facilities for exhaust gas treatment or cannot operate
416 facilities normally were to be discontinued. Petrochemical and chemical enterprises were forbidden to turn on/off
417 for operation or maintenance. (3) Strictly control motor vehicle pollution: in the core areas in Zhejiang province,
418 motor vehicle restrictions were implemented, which means that low-speed trucks were forbidden to pass except for
419 people's livelihood-related activities. Vehicles which had not obtained valid qualifications for environmental
420 inspection were prohibited on the road. (4) Control dust pollution: Controlled work sites were suspended in key
421 areas and control areas. Dust materials were forbidden to be transported within key neighbourhoods. Dust control
422 measures were implemented on renovation operations at ports, docks, railway stations and commercial concrete
423 mixing stations and on materials storage yards. (5) Control other sources of pollution: in key areas and control areas,
424 oil storage facilities, gas stations or tank trucks which were not equipped with facilities for recovery of oil and gas
425 or facilities that could not operate normally were forbidden to sell or transport oil products. Open air barbecue,
426 garbage burning or straw burning in the open air were prohibited. All the primary schools, secondary schools,
427 kindergartens, institutions and public institutions in Jiaying were given a three-day vacation.

428 Zhejiang province initiated control measures on December 8, which included: First, strictly control emissions
429 from coal-burning power plants through the use of low-sulphur coal and production restrictions; Second, cut
430 emissions from key enterprises through measures such as production restriction and suspension; Third, all
431 enterprises that cannot meet the emission standards in a stable way shall be discontinued; Fourth, rubbish and straw
432 burning shall be strictly supervised. During the period, 109 coal-burning power plants in total had imposed
433 production restrictions in Hangzhou, Ningbo, Huzhou, Jiaying, Shaoxing and Jinhua. A total of 1331 key enterprises
434 reduced their operations among which 720 were restricted from production. Similarly, 3950 key controlled
435 construction sites were suspended from operation, 83 concrete enterprises were restricted from production, 444 sites
436 of straw burning were regulated, and 296 "black chimneys" were inspected.

437 As a neighbouring city, the Shanghai municipality released their Action Plan for Air Quality Control at the
438 World Internet Conference in 2015, focusing on key areas such as Jinshan district, Fengxian district, Shanghai
439 chemical industry and Shanghai petrochemical industry, and implemented emissions controls on petrochemical,
440 steel, chemical, coating and printing industries. On the morning of December 14, temporary control measures were
441 initiated. In total, 313 key enterprises and over 1000 key buildings and municipal sites were under the control of the
442 city, more than 320 construction sites were suspended from operation, and over 600 yard terminals strengthened
443 dust control measures. The ban on Yellow Label cars and the restriction on diesel vehicles within the middle ring
444 in Shanghai were implemented. On the morning of December 15, the Yellow Alert emergency plan was launched.
445 On that day, 643 key enterprises were controlled, among which 178 were restricted from production. In total, 174



446 construction sites, 310 demolition sites, 66 municipal road sites and 44 dock yards were suspended from operation,
447 along with an increase in rinsing and cleaning frequency for 2060 roads to reduce fugitive dust emissions.

448 Jiangsu province expanded key areas for air quality control from two districts in Suzhou (Wujiang and
449 Wuzhong) to three cities (Suzhou, Wuxi and Changzhou). In total, 8 power plants adopted high-quality coals in
450 Suzhou, another 8 power plants limited their production by 30%, and over 60 key enterprises took measures such
451 as restricting the production and shutting down of coal-fired boilers. Construction work sites in control areas were
452 suspended from operation. In Wuxi, thermal power enterprises adopted high-quality low-sulphur coals, electricity
453 power enterprises and 82 key enterprises were restricted or suspended from production.

454 In Anhui province, three control areas (Ma'anshan, Xuancheng and Wuhu) and 6 extension areas including
455 Anhui all developed and implemented control programs. During the campaign, 23 coal-fired power plants were
456 controlled for low emission, 126 enterprises were restricted from production and 287 construction work sites were
457 controlled. Among which, 3 cement enterprises in Xuancheng limited their production by 30%, another 3 cement
458 enterprises and 2 chemical enterprises limited their production by 50%, 9 construction sites were suspended from
459 operation, lime production and process enterprises were discontinued, quarrying and stone transportation were
460 prohibited, and other non-coal mines were discontinued.

461 During the campaign, the YRD region was frequently affected by unfavourable weather conditions such as
462 pollution transportation from the north. There were four distinct meteorological regimes, which occurred in Jiaying
463 and its surrounding cities. Therefore, some cities further took stricter pollution reduction measures. Shanghai
464 municipality started temporary control of heavy pollution on December 14 and initiated the yellow warning for
465 heavily polluted weather on December 15. On that day, 643 key enterprises were controlled, 178 enterprises were
466 restricted from production, over 1000 dusty construction sites were discontinued and the rinsing and cleaning
467 frequency increased for over 2000 roads. Starting from December 11 in Jiangsu province, 1260 enterprises were
468 restricted from production, 1429 enterprises were discontinued, and all construction sites in control areas were
469 suspended from operation. Emergency control measures were initiated on December 15, strengthening control
470 efforts for industries, work sites and motor vehicles.

471 **3.3.2 Emissions reduction estimation**

472 Based on the implementation of control measures in all areas during the conference and whether each area had
473 effectively implemented control measures on December 8-18, regional emission reductions have been assessed. It
474 is estimated that emission reductions of SO₂, NO_x, PM_{2.5} and VOCs caused by production restriction in regional
475 industrial enterprises are 2867.8 tons, 3064.7 tons, 2165.5 tons and 5055.4 tons, respectively. Emission reductions



476 of various pollutants caused by the restrictions on motor vehicle traffic are estimated as 4.7 tons of SO₂, 326.9 tons
477 of NO_x, 36.1 tons of PM_{2.5} and 452.5 tons of VOCs. Emission reduction of PM_{2.5} caused by dust control was
478 estimated as 266.0 tons. Therefore, it can be seen that emission reductions mainly come from industrial sources,
479 while motor vehicle restrictions contributed greatly to emission reductions of NO_x and VOCs, and dust control
480 contributed 10% to emission reductions of PM_{2.5}.

481 When looking at specific industries, the electricity power industry contributed most to the emission reductions
482 of SO₂ and NO_x at 49.7% and 46.9%, respectively, followed by the chemical industry, building materials industry,
483 steel industry and petrochemical industry with a total contribution from all four sectors to emission reductions of
484 SO₂ and NO_x of 42.0% and 47.2%, respectively. For PM_{2.5}, the building materials industry contributed the most at
485 62.0%, followed by steel and processing industry, power industry and non-ferrous smelting and process industry
486 with a contribution of 14.3%, 13.1% and 8.1%, respectively. For VOCs, the emission reduction sectors are mainly
487 chemical, petrochemical and machinery manufacturing sectors with a total contribution of 65.7% and individual
488 contributions of 25.1%, 23.2% and 17.4%, respectively. In addition, metal products processing, building materials
489 and steel and processing sectors also contributed significantly to emission reductions of 13.4%, 8.0% and 6.5%,
490 respectively.

491 In terms of the regional distribution of emission reductions, Jiaxing, Hangzhou, Suzhou and Shaoxing have the
492 largest contribution of around 80%. These four cities contribute 87% to the total emission reduction of PM_{2.5}.

493 Combing all control measures, total emission reductions of SO₂, NO_x, PM_{2.5} and VOCs are estimated as 2872.5
494 tons, 3391.6 tons, 2467.6 tons and 5507.9 tons, respectively, which accounts for 10%, 9%, 10% and 11%,
495 respectively, of the total urban emissions. It is worth mentioning that if we consider the emergency emission
496 reduction measures for heavy pollution during the campaign, the amount of emission reduction for all pollutants
497 and the proportion of their emission reductions would be even larger. Table 4 shows the percentage and the amount
498 of emission reductions for pollutants under various control measures.

499
500

Table 4 Emission reduction estimations for various control measures

Province	City	Sector	Amount of emission reduction (tons)				Percentage of reduction			
			SO ₂	NO _x	PM _{2.5}	VOCs	SO ₂	NO _x	PM _{2.5}	VOCs
	Jiaxing		925.6	709.5	462.3	1872.7	56%	58%	64%	80%
	Huzhou		414.8	585.6	602.5	514.0	46%	37%	47%	53%
Zhejiang	Hangzhou	Industries	657.2	654.1	476.2	1043.2	36%	42%	59%	33%
	Ningbo	and	59.1	65.3	107.5	84.0	32%	30%	37%	33%
	Shaoxing	enterprises	365.9	414.8	403.9	678.7	34%	38%	62%	31%
Shanghai	Shanghai		253.6	368.7	83.6	796.1	9%	7%	6%	8%
Jiangsu	Suzhou		89.4	34.9	10.2	11.4	3%	1%	1%	1%



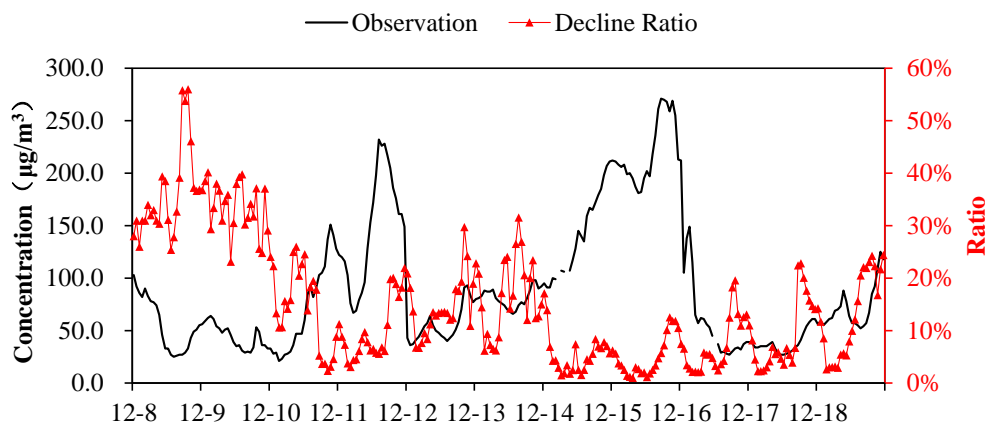
	Wuxi		94.4	163.0	10.2	55.3	12%	10%	1%	5%
Anhui	Xuancheng		7.8	68.8	9.1	0.0	15%	42%	28%	0%
	Sub-total		2867.8	3064.7	2165.5	5055.4	23%	19%	27%	19%
	Jiaxing	Motor vehicles	2.3	157.7	16.4	211.3	46%	53%	38%	25%
Zhejiang	Huzhou		0.7	48.4	6.2	81.0	23%	24%	19%	12%
	Hangzhou		1.7	120.8	13.5	160.2	8%	15%	20%	20%
	Sub-total		4.7	326.9	36.1	452.5	15%	25%	25%	19%
	Jiaxing	Dust control	/	/	119.5	/	/	/	100%	/
	Huzhou		/	/	11.1	/	/	/	10%	/
Zhejiang	Hangzhou		/	/	26.6	/	/	/	10%	/
	Ningbo		/	/	28.8	/	/	/	5%	/
	Shaoxing		/	/	5.8	/	/	/	5%	/
Shanghai	Shanghai		/	/	69.3	/	/	/	6%	/
Jiangsu	Suzhou		/	/	2.7	/	/	/	1%	/
	Wuxi		/	/	1.8	/	/	/	1%	/
Anhui	Xuancheng	/	/	0.4	/	/	/	1%	/	
	Sub-total	/	/	266.0	/	/	/	9%	/	
	In total	2872.5	3391.6	2467.6	5507.9	10%	9%	10%	11%	

501

502 3.4 Quantitative estimates of the contribution of meteorological and control measures to air quality 503 improvement

504 3.4.1 PM_{2.5} concentration improvement in Jiaxing

505 The WRF-CMAQ air quality model, combined with observations, was used to evaluate the reduction in PM_{2.5}
 506 concentration in Jiaxing due to the emission reductions achieved through the campaign. This analysis utilized two
 507 model simulations to assess the impact of the emission reductions: 1) a baseline scenario, which utilized an
 508 uncontrolled emission inventory (i.e., the emissions that would have occurred without the campaign), and 2) an
 509 emission inventory, which reflects the emission reductions achieved by the campaign. Figure 13 shows the time
 510 series of PM_{2.5} observed concentrations and the percent change in PM_{2.5} after the air quality control measures were
 511 implemented. It can be seen that the reduction in PM_{2.5} concentrations in Jiaxing varies with time. The reduction in
 512 PM_{2.5} was the most significant on December 8-9 with a maximum reduction of 56%. The percent reduction in hourly
 513 PM_{2.5} during the conference (December 16-18) ranged between 2%-24%, while the average decrease in PM_{2.5}
 514 concentration was 5.8 µg/m³ with an average improvement of about 12.9%. During the campaign from December 8
 515 to December 18, average PM_{2.5} concentrations decreased by 10.5 µg/m³ with an average decrease of 14.4%.
 516 However, Although there are many control strategies implemented, the effects during 12/14-12/16 are low. As
 517 described in section 3.1.2, the prevailing wind direction during this period is NW, and Jiaxing experienced a heavy
 518 pollution process with the transit and transportation of strong cold air. Therefore, we can not see obvious effect
 519 without strong upwind precursor emissions reductions.



520

Fig. 13 Time series of observed $PM_{2.5}$ and the percent reduction resulting from the implementation of air quality control measures

522

Figure 14 shows the reduction in daily average $PM_{2.5}$ concentrations in Jiaxing resulting from the emission reductions associated with the Action Plan for Air Quality Control at the World Internet Conference. As can be seen from the figure, the improvement in $PM_{2.5}$ before the conference (December 8 and 9) was relatively significant, with a daily average decline of roughly 31% and 35%, respectively, which corresponds to a decrease of around $17 \mu g/m^3$. The reduction in $PM_{2.5}$ on December 14-15, two of the days with some of the highest observed $PM_{2.5}$, was relatively low at around 6%, while daily average $PM_{2.5}$ concentrations on those days decreased by around $10.0 \mu g/m^3$. The magnitude of emission reductions during those two time periods was basically the same, so it's likely that the observed difference in $PM_{2.5}$ levels was the result of meteorological differences, and in particular, enhanced transport of polluted air into Jiaxing from December 14 to 15. Overall, under the influence of regional control measures for emission reductions from December 8 to December 18, $PM_{2.5}$ daily average concentration decreased by 5.5%-34.8% with an average of 14.6% or $10 \mu g/m^3$.

523

524

525

526

527

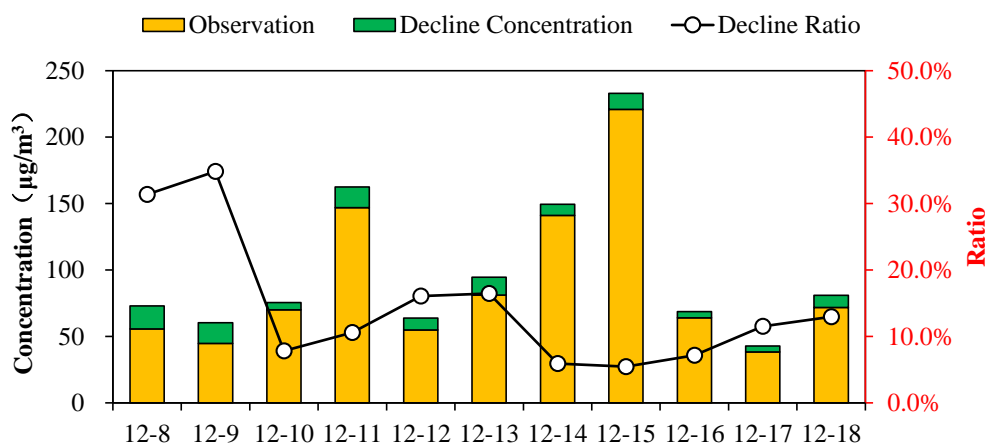
528

529

530

531

532



533

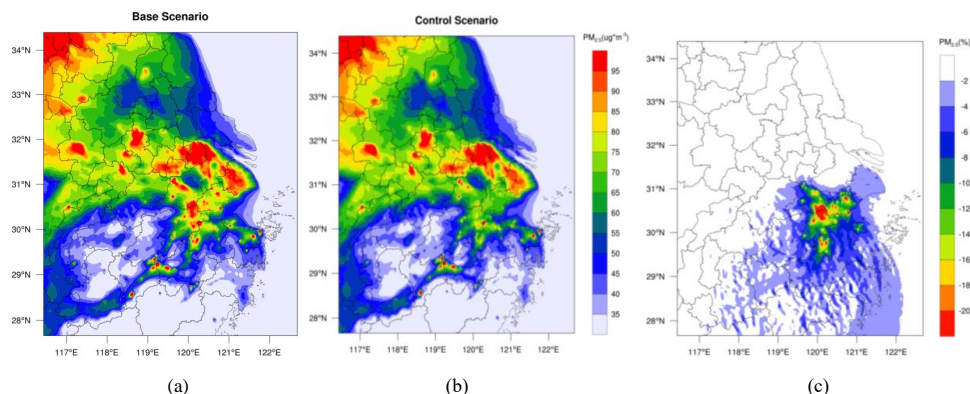
534

Fig.14 Percent reduction in $PM_{2.5}$ resulting from the control measures



535 3.4.2 PM_{2.5} concentration improvement across regions

536 Figure 15 shows the spatial distribution of PM_{2.5} concentrations in the Yangtze River Delta region from
537 December 8 to December 18 in the baseline scenario and the campaign scenario. As can be seen from the figure,
538 southern Jiangsu, Shanghai and northern Zhejiang in the central YRD region had relatively high PM_{2.5}
539 concentrations, which is consistent with the typically more serious pollution levels in autumn and winter in the YRD
540 region. Under the influence of regional control measures, PM_{2.5} average concentrations declined significantly in
541 Jiaxing, Hangzhou and Huzhou, especially at the junction of these three cities, with a slight improvement in central
542 southern Zhejiang too. The average percent reduction in PM_{2.5} concentrations in Jiaxing, Hangzhou and Huzhou
543 was about 6%-20%. Meanwhile, given that the prevailing winds are north-westerly in winter, there was also some
544 improvement in central and southern Zhejiang.



545

546

547

548

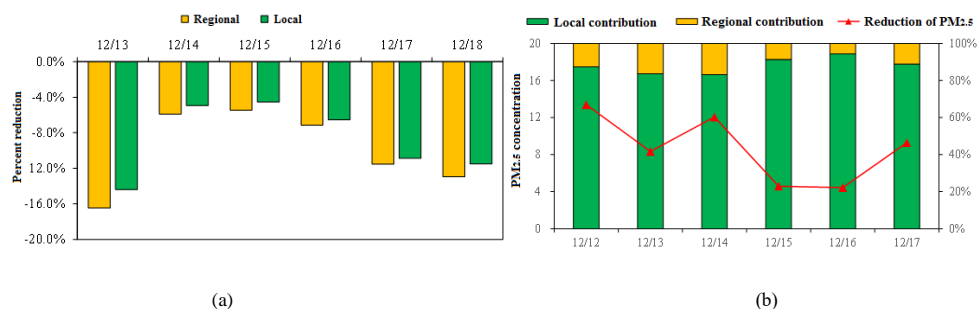
Fig. 15 Spatial distribution of PM_{2.5} concentrations in the Yangtze River Delta region under the baseline scenario (a) and the campaign scenario (b), and the percent reduction in PM_{2.5} throughout the YRD region (c)

549

3.4.3 Regional contributions of PM_{2.5} concentration improvement in Jiaxing

550 Figure 16(a) shows the percent reduction in PM_{2.5} daily average concentrations from December 13 to
551 December 18 after control measures were implemented in Jiaxing and regionally. The reduction in PM_{2.5} was the
552 results of both local controls, as well as regional controls which reduced pollution in the air masses transported into
553 Jiaxing. Overall, modelling suggests that the regional controls reduced PM_{2.5} levels in Jiaxing between 5.5%-16.5%
554 (9.9% average), while local control measures contributed 4.5%-14.4%, with an average of 8.8%.

555 Figure 16(b) shows the average contribution of local emissions reductions in Jiaxing and in the YRD region
556 over the entire campaign (Dec.13-18), as well as the corresponding improvement in PM_{2.5} levels in Jiaxing. During
557 this period, PM_{2.5} daily average concentration declined by 4-13 µg/m³, while there were differences in the
558 contribution of regional remission reductions and local emission reductions in Jiaxing during different periods.
559 Overall, local control measure in Jiaxing had the largest impact on PM_{2.5} levels and accounted for 89% of the decline
560 in PM_{2.5}, while regional control measures contributed the remaining 11%.



561

562

563 Fig. 16 Percent reduction in daily average PM_{2.5} concentrations from December 13 to December 18 after implementation of the
 564 control measures across the region and in Jiaying (a) and Contribution of local and regional emissions reductions in Jiaying, and the
 565 resulting improvement of daily average PM_{2.5} concentrations in Jiaying (b)

566 3.5 Optimisation scenario analysis of regional linkage control measures

567 3.5.1 Optimization scenario settings

568 In order to further analyse the optimisation potential of air quality control measures for major events and
 569 enhance the effectiveness of the control measure scheme design, three control measure optimisation scenarios have
 570 been set on the basis of the evaluation scenario (Base) after the implementation of air quality control measures
 571 during the conference. These scenarios include local emission reductions in Jiaying under stagnant meteorological
 572 conditions, where local emission accumulation is the main contributor to the pollution process (Sc.1), and the
 573 emission reduction scenario where transport of polluted air masses into Jiaying is a major contributor to the PM_{2.5}
 574 levels in Jiaying. In order to investigate the transport processes further, the latter scenario was further divided into
 575 a scenario 24 hours in advance (Sc.2) and a scenario 48 hours in advance (Sc.3). Table 5 describes the details of
 576 each scenario.

577

578

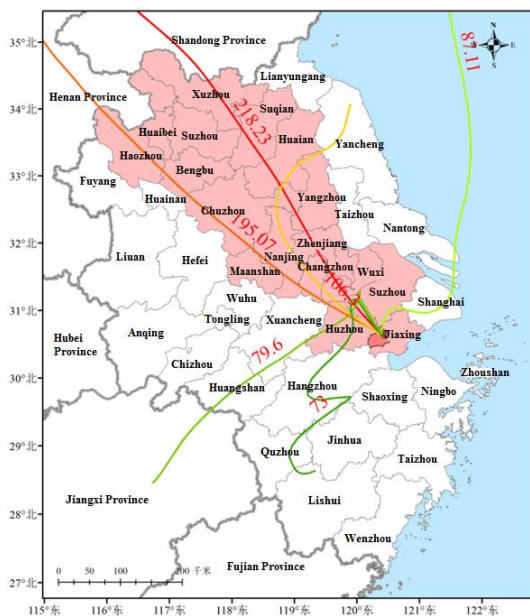
Table 5 Control measure optimization scenario settings

Scenario name	Scenario settings	Emission reduction regions	Emission reduction measures	Starting time
Base	Regional emission reduction	All the cities and areas involved in the campaign scheme	All control measures mentioned in the campaign scheme	December 8
Sc.1	Local emission reduction in Jiaying	Jiaying	Control measures in Jiaying mentioned in the campaign scheme	December 8
Sc.2	Emission reduction through transportation channels 24 hours in advance	Cities located in the northwest transportation channel of Jiaying	Cut down industrial sources by 30%	December 13
Sc.3	Emission reduction through transportation channels 48 hours in advance	Cities located in the northwest transportation channel of Jiaying	Cut down industrial sources by 30%	December 12

579 Figure 17 shows the cities that primarily influence the polluted air masses transported into Jiaying, where the



580 transport channels were determined through backward trajectory analysis. These cities include Huzhou in Zhejiang
581 province, Suzhou, Wuxi, Changzhou, Nanjing, Zhenjiang, Huai'an, Suqian and Suzhou in Jiangsu province and
582 Suzhou, Huaibei, Bozhou, Bengbu, Chuzhou and Ma'anshan in Anhui province. Each of these cities took measures
583 to reduce emissions by limiting production from industry industries by 30%.



584
585

Fig. 17 Cities involved in the transportation channel and the emission reduction channel

586 The WRF-CMAQ modelling system was used to analyse and compare the air quality improvement effect under
587 different pollution process in four scenarios.

588 3.5.2 Analysis of optimization scenario effects

589 In order to evaluate the effect of the different starting time for the same control measures, and the same starting
590 time for local and regional control measures, we conducted four scenarios. Figure 18 shows the percent reduction
591 in daily average PM_{2.5} concentrations in Jiaxing City from December 13 to December 18 under the regional emission
592 reduction scenario, the Jiaxing local emission reduction scenario and the transportation channel emission reduction
593 scenario. Overall, there are differences in the distribution of PM_{2.5} under the different scenarios. The air quality
594 improvement due to the regional emission reductions was higher than that of local emission reductions in Jiaxing,
595 and lower than that of channel emission reductions.

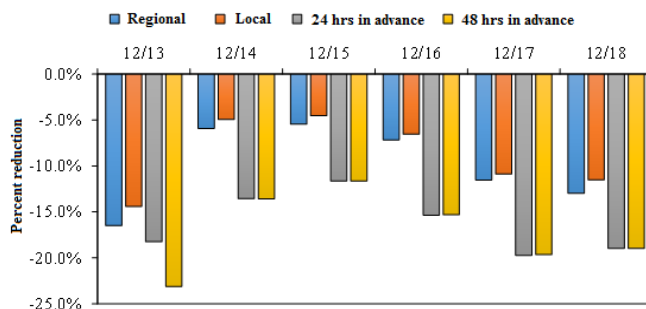


Fig. 18 Decline rates of PM_{2.5} daily average concentrations in Jiaxing under different scenarios

596

597

598 (1) Effect of local emission reductions in Jiaxing

599 By comparing the effect of local emission reductions in Jiaxing (Sce.1) and the effect of regional emission
600 reductions (Base), we can see that PM_{2.5} daily average concentrations in Jiaxing declined by around 5.5%-16.5%
601 under the regional emission reduction plan (regional emission plan including the local emissions control) from
602 December 13 to December 18 and by around 4.5%-14.4% under the local emission reduction plan. Local emission
603 reductions in Jiaxing contributed 83%-94% to the emission reduction effect. Therefore, local emission reduction in
604 Jiaxing is the key factor in improving the local air quality.

605 Compared with the channel emission reduction scenario 24 hours in advance (11.6%-18.2%), local emission
606 reductions also contributed more than 50% to the improvement effect on December 13, 17 and 18. Therefore, local
607 emission reductions contributed most to the air quality improvement effect in Jiaxing, indicating that local areas are
608 still the most important control areas during the campaign.

609 (2) Effect of emission reductions through transportation channels

610 As mentioned above, during the large-scale transport of heavily polluted air masses into the Yangtze River
611 Delta region from December 14 to December 15, the PM_{2.5} pollution in Jiaxing was significantly affected. Under
612 the local emission reduction scenario (Sce.1) and the regional linkage emission reduction scenario (Base), PM_{2.5}
613 daily average concentrations in Jiaxing decline by only 4.5%-5.9%. If a 30% reduction in emissions from industrial
614 sources in the upwind transportation channel is implemented, PM_{2.5} daily average concentrations in Jiaxing declined
615 by 11.6%-13.6%, while local emission reductions contributed less than 40% to the improvement of PM_{2.5}. Therefore,
616 to reduce PM_{2.5} under these large-scale transport conditions, in addition to intensifying local emission reduction
617 efforts, it is more effective to prevent and control such pollution by adopting emission reductions of industrial
618 sources over key transportation channels, especially for elevated sources.

619 In this study, the main transportation channel involved is the northwest transportation channel in control areas,
620 which basically represents the typical winter transportation channel in the region. A well-designed management



621 plan for the main transportation channel is necessary to ensure the air quality in autumn and winter is improved, in
622 addition to reducing local emissions.

623 (3) Effect of the starting time for channel emission reductions

624 According to the comparisons between the emission reduction scenario 24 hours in advance (Sce.2) and the
625 emission reduction scenario 48 hours in advance (Sce.3) during the large-scale PM_{2.5} transport, we can see that if
626 we take December 13 as the target and adopt channel emission reductions 48 hours in advance, PM_{2.5} daily average
627 concentrations will decline by 23.1% when compared to the baseline scenario, which is significantly better than the
628 improvement achieved by the emission reduction scenario 24 hours in advance (18.2%). Therefore, early measures
629 to reduce emissions will lead to the improvement of air quality.

630 If we focus on the conference period (December 16-18), PM_{2.5} daily average concentrations will both decline
631 by 15.3%-19.7% under the two channel emission reduction scenarios, indicating a close improvement effect.
632 Therefore, during the pollution process when local emissions are the main contributor, local emission reductions
633 should be the top priority with no difference between channel reductions 24 hours in advance and 48 hours in
634 advance. If transportation emissions are the main contributor to the pollution, adopting channel reductions 48 hours
635 in advance can bring about more improvement effect than 24 hours in advance.

636 3.6 Comparisons with other air quality guarantee events

637 Besides the 2nd World Internet Conference, China has hosted many other mega events in recent years, like
638 2008 Beijing Olympics, 2010 Guangzhou Asian Games, 2014 Beijing APEC, 2014 Nanjing Youth Olympics and
639 2015 Victory Parade. To guarantee the better air quality and protect people's health, local government had
640 implemented numerous short-term stringent strategies to guarantee air quality during these events, which
641 significantly reduced the emissions and concentrations of air pollutants in these cities and surrounding area. Through
642 banning yellow-label vehicles from driving, stopping all construction activities and requiring heavily polluting
643 factories to reduce their operating capacities or completely shut down during the 2008 Olympics, the mean
644 concentrations of SO₂, PM_{2.5} and NO₂ in Beijing and its surrounding area were reduced by 51.0%, 43.7% and 13%
645 compared to the period before Olympics, and concentrations of O₃, SO₂, CO and NO_x decreased 23%, 61%, 25%
646 and 21% compared to previous years (Wang, et al., 2009; Wang, et al., 2010). During the 2010 Asian Games, the
647 Guangzhou government made great efforts to improve the air quality, such as controlling emissions from industries
648 and transportation restrictions, requiring vehicles to drive only on alternate days depending on license plate numbers,
649 and prohibiting all construction activities. The emissions of SO₂, NO_x, PM₁₀, PM_{2.5} and VOCs were reduced by
650 41.1%, 41.9%, 26.5%, 25.8% and 39.7%, respectively, leading to a dramatic decrease on concentrations of SO₂,



651 NO₂, PM₁₀ and PM_{2.5} in Guangzhou (Liu, et al., 2013). During the 2014 Asia-Pacific Economic Cooperation
 652 (APEC) period, the average concentrations of PM_{2.5}, PM₁₀, SO₂ and NO₂ decreased by 47%, 36%, 62% and 41%
 653 respectively by controlling emissions from traffic, industry, construction sites and so on (Tang, et al., 2015; Li, et
 654 al., 2016; Wang, et al., 2016; Sun, et al., 2016; Wang, et al., 2015). During 2014 Nanjing Youth Olympics and 2015
 655 Victory Parade, the local governments also successfully improved air quality by carrying out many air pollution
 656 control measures including relocating some heavily polluting enterprises, encouraging natural gas instead of coal-
 657 fired boilers and domestic stoves, limiting the use of cars and so on (Chen, et al., 2017; Han, et al., 2016). Also, 22
 658 surrounding cities in the YRD region were asked to cooperate with Nanjing to close industries with high pollution
 659 emissions. Some research papers demonstrate that, the mean concentrations of PM_{2.5}, PM₁₀, SO₂, NO₂, CO and O₃
 660 in Nanjing during the Youth Olympics decreased by 35.92%, 36.75%, 20.40%, 15.05%, 8.54% and 47.15%,
 661 respectively, compared with the average levels in July 2014 (Qi, et al., 2016). The emission reductions for SO₂,
 662 NO_x, PM₁₀, PM_{2.5}, VOCs during the Victory Parade were 36.5%, 49.9%, 50.3%, 49.0% and 32.4%, respectively.
 663 These results show that stringent emission reduction strategies had greatly relief the air pollution of these cities
 664 including their surrounding area, and further improve their air quality through regional joint control measures.

665 Table 6 Summary of control strategies taken during different periods

Periods	Control area	Control policies	Main achievements or targets
Beijing Olympics, 2008	Jing-jin-ji area Inner Mongolia, Shanxi, Shandong	Yellow-label vehicles were banned from driving; personal vehicles were taken off the roads through the alternative day-driving scheme; all construction activities were halted; power plants were asked to use cleaner fuels and reduce their emissions by 30% from their levels; heavily polluting factories were ordered to reduce operating capacities or completely shut downs.	The emissions of SO ₂ , NO _x , CO, VOCs, and PM ₁₀ were reduced by 14%, 38%, 47%, 30% and 20% respectively; the concentrations of fine and coarse particulate matter were reduced by 35–43%.
Beijing APEC, 2014	Jing-jin-ji area Shanxi, Inner Mongolia, Shandong	Reducing or stopping production in factories, halting production on construction sites, imposing the odd-even traffic rule for vehicles, and strengthening road cleaning measures.	Average concentrations of SO ₂ , NO ₂ , PM ₁₀ and PM _{2.5} decreased by 62%, 41%, 36%, and 47%, respectively.
Nanjing Youth Olympics, 2014	Nanjing	2630 construction sites were halted; heavy-industry factories were required to reduce manufacturing by 20%; high-emission vehicles were not allowed to drive on the road; open space barbecue restaurants were closed; over 900 electric buses and 500 electric taxis have been put into operation.	The mean concentrations of PM _{2.5} , PM ₁₀ , SO ₂ , NO ₂ , CO and O ₃ decreased by 35.92%, 36.75%, 20.40%, 15.05%, 8.54% and 47.15%.
Beijing	Jing-jin-ji	Over 111 businesses with high emissions	The emission reductions were 36.5%



Victory Parade, 2015	area, Shanxi, Shandong, Inner Mongolia, Henan	were required to stop or limit their production; the odd-even rule was implemented to restrict traffic emissions; 80% of government vehicles were prohibited on roads; trucks transporting mud and stone as well as heavy-emission vehicles were prohibited from roads; over 10000 enterprises were closed or ordered to limit production, and about 9000 construction sites were shut down.	for SO ₂ , 49.9% for NO _x , 50.3% for PM ₁₀ , 49.0% for PM _{2.5} and 32.4% for VOCs in Beijing.
----------------------------	---	--	---

666

667 **4 Conclusions**

668 **(1) The effect of restricting production in industrial enterprises is remarkable.** The power industry and
669 related industrial enterprises in Jiaxing cut down SO₂ and NO_x emissions by over 50%, while the building materials
670 industry, smelting industry and other industrial enterprises cut down PM_{2.5} emissions by 63%, contributing greatly
671 to the reduction of primary PM_{2.5} concentrations. The petrochemical industry, chemical industry and other related
672 industrial enterprises cut down VOCs emission by 66% in total, contributing greatly to the reduction of PM_{2.5}
673 formed through the conversion of precursor species. The observation data of PM_{2.5} components suggest that the
674 relative contribution of secondary components dropped significantly during the conference. Production restriction
675 or suspension for industrial enterprises is the main contributor to emission reductions for various pollutants during
676 the campaign, which resulted in the largest improvement in air quality.

677 **(2) Motor vehicle pollutant emissions declined significantly.** In Jiaxing, motor vehicle restrictions were fully
678 implemented during heavy pollution days, temporary traffic control was implemented during certain periods, and
679 enterprises and institutions had a three-day vacation during the conference. Emission reduction rates for various
680 pollutants from motor vehicle emissions were around 40%-50%. Motor vehicle emission reduction measures
681 contributed to the total emission reductions of nitrogen oxides by 18.2%, fine particles by 3.4% and volatile organic
682 compounds by 10.1%.

683 **(3) The effect of dust control measures is remarkable.** During the conference, all the work sites in Jiaxing
684 and 3950 work sites in total in Zhejiang province were suspended from operation. Measures of increasing frequency
685 for road cleaning activities greatly lowered the dust emissions. Speciation of the measured PM_{2.5} suggest that the
686 mass concentration of crust material, which is greatly affected by dust, decreased by 14% compared to
687 measurements after the conference, indicating the effectiveness of dust control measures.

688 **(4) Regional linkage between surrounding areas played an important role.** PM_{2.5} is a typical regional air
689 pollutant, with obvious regional transportation characteristics. In accordance with the requirements of the campaign
690 scheme, eight cities around Jiaxing have actively implemented emissions reduction measures. During the campaign,



691 PM2.5 concentrations in eight surrounding cities and south-eastern Zhejiang also declined with obvious regional
692 synergies.

693 It is worth noting that the implementation of control measures has also had a negative impact on the economy
694 and the society in the short term while improving the air quality. For example, production restriction or suspension
695 on a large number industrial enterprises were taken at great economic costs, and motor vehicle restriction had a
696 large impact on the society.

697 **(5) Suggestions on emission reduction plans:** Local emission reductions shall be supplemented by regional
698 linkage. Assessment results show that local emission reductions play a key role in ensuring air quality. Therefore,
699 it is recommended that a synergistic emission reduction plan between adjacent areas with local pollution emission
700 reductions as the core part should be established and strengthened, and emission reduction plans for different types
701 of pollution through a stronger regional linkage should be reserved. Strengthen the pollution reduction in the upper
702 reaches along the transportation channel. It is especially crucial to enhance pollution emission reductions in the
703 upper reaches of the channel since long-distance transport of pollution is a problem. This is especially true for key
704 industrial sources and elevated sources. Considering that polluted air mass transportation is more frequent in winter,
705 it is necessary to develop emission reduction plans for different pollution transportation channels, combined with
706 forecasting and warning mechanisms which could be initiated on time.

707

708 **Acknowledgements.**

709 This study was financially supported by the “Chinese National Key Technology R&D Program” via grant No.
710 2014BAC22B03 and the National Natural Science Foundation of China (NO. 41875161). We also thank the Joint
711 pollution control office over the Yangtze River Delta region for co-ordinating the data share.

712 **References**

713 Borge, R., Lumberras, J., Vardoulakis, S., et al.: Analysis of long-range transport influences on urban PM10 using two-stage
714 atmospheric trajectory clusters, *Atmos. Environ.*, 41, 4434-4405, 2007.

715 Burr, M. J., and Zhang, Y.: Source apportionment of fine particulate matter over the Eastern U.S. Part I: source sensitivity simulations
716 using CMAQ with the Brute Force method, *Atmos. Pollut. Res.*, 2, 300-317, 2011.

717 Chen, P. L., Wang, T. J., Lu, X. B., et al.: Source apportionment of size-fractionated particles during the 2013 Asian Youth Games and
718 the 2014 Youth Olympic Games in Nanjing, China, *Sci. Total Environ.*, 579,860-870, 2017.

719 Chang, J. S., Brost, R. A., Isaksen, I. S. A., Madronich, S., Middleton, P., Stockwell, W. R., and Walcek, C. J.: A 3-DIMENSIONAL
720 EULERIAN ACID DEPOSITION MODEL - PHYSICAL CONCEPTS AND FORMULATION, *J. Geophys. Res.*, 92, 14681-14700,
721 1987.



- 722 Chou, M. D., and Suarez, M. J.: A solar radiation parameterization (CLIR-AD-SW) for atmospheric studies, 1999.
- 723 CAI-Asia: “Blue Skies at Shanghai EXPO 2010 and Beyond: Analysis of Air Quality Management in Cities with Past and Planned
724 Mega-Events: A Survey Report.” Pasig City, Philippines, 2010.
- 725 CAI-Asia: “Nanjing YOG 2014 Home” Pasig City, Philippines, 2014.
- 726 Ek, M. B.: Implementation of Noah land surface model advances in the National Centers for Environmental Prediction operational
727 mesoscale Eta model, *J. Geophys. Res.*, 108(D22), 2003.
- 728 Fu, X., Cheng, Z., Wang, S., Hua, Y., Xing, J., and Hao, J.: Local and Regional Contributions to Fine Particle Pollution in Winter of
729 the Yangtze River Delta, China, *Aerosol Air. Qual. Res.*, 16, 1067-1080, 2016.
- 730 Guenther, A. B., Jiang, X., Heald, C. L., Sakulyanontvittaya, T., Duhl, T., Emmons, L. K., and Wang, X.: The Model of Emissions of
731 Gases and Aerosols from Nature version 2.1 (MEGAN2.1): an extended and updated framework for modeling biogenic emissions,
732 *Geosci. Model Dev.*, 5, 1471-1492, 2012.
- 733 Grell, G. A., and Dévényi, D.: A generalized approach to parameterizing convection combining ensemble and data assimilation
734 techniques, *Geophys. Res. Lett.*, 29(14), 587-590, 2002.
- 735 Han, X. K., Guo, Q. J., Liu, C. Q., et al.: Effect of the pollution control measures on PM_{2.5} during the 2015 China Victory Day Parade:
736 Implication from water-soluble ions and sulfur isotope, *Environ. Pollut.*, 218, 230-241, 2016.
- 737 Hu, J. L., Wang, Y. G., Ying, Q., et al.: Spatial and temporal variability of PM_{2.5} and PM₁₀ over the North China Plain and the
738 Yangtze River Delta, China, *Atmos. Environ.*, 95, 598-609, 2014.
- 739 Hu, J. L., Wu, Li., Zheng, B., et al.: Source contributions and regional transport of primary particulate matter in China, *Environ. Pollut.*,
740 207, 31-42, 2015.
- 741 Hsu, Y. K., Holsen, T. M., and Hopke, P. K.: Comparison of hybrid receptor models to locate PCB sources in Chicago, *Atmos. Environ.*,
742 37, 545-562, 2003.
- 743 Hong, S. Y.: A new vertical diffusion package with an explicit treatment of entrainment processes, *Mon. Weather Rev.*, 134, 2318,
744 2006.
- 745 Huang, C., Chen, C. H., Li, L., Cheng, Z., Wang, H. L., Huang, H. Y., Streets, D. G., Wang, Y. J., Zhang, G. F., and Chen, Y. R.:
746 Emission inventory of anthropogenic air pollutants and VOC species in the Yangtze River Delta region, China, *Atmos. Chem. Phys.*,
747 11, 4105-4120, 2011.
- 748 Huang, Y. M., Liu, Y., Zhang, L. Y., et al.: Characteristics of Carbonaceous Aerosol in PM_{2.5} at Wanzhou in the Southwest of China,
749 *Atmosphere*, 9, 37, 2018,.
- 750 Jiang, C., Wang, H., Zhao, T., et al.: Modeling study of PM_{2.5} pollutant transport across cities in China’s Jing–Jin–Ji region during a
751 severe haze episode in December 2013, *Atmos. Chem. Phys.*, 15, 5803–5814, 2015.
- 752 Kang, H. Q., Zhu, B., Su, J. F., et al.: Analysis of a long-lasting haze episode in Nanjing, China, *Atmos. Res.*, 120–121, 78–87, 2013.



- 753 Kelly, F. J., and Zhu, T.: Transport solutions for cleaner air, *Science*, 352, 934–936, 2016.
- 754 Li, L., An, J. Y., Zhou, M., Yan, R. S., Huang, C., Lu, Q., and Chen, C. H.: Source apportionment of fine particles and its chemical
755 components over the Yangtze River Delta, China during a heavy haze pollution episode, *Atmos. Environ.*, 123, 415–429, 2015.
- 756 Li, R. P., Mao, H. J., Wu, L., et al.: The evaluation of emission control to PM concentration during Beijing APEC in 2014, *Atmos.*
757 *Pollut. Res.*, 7 (2), 363–369, 2016.
- 758 Liu, H., Wang, X. M., Zhang, J. P., et al.: Emission controls and changes in air quality in Guangzhou during the Asian Games, *Atmos.*
759 *Environ.*, 76, 81–93, 2013.
- 760 Lv, B. L., Liu, Y., Yu, P., et al.: Characterizations of PM_{2.5} Pollution Pathways and Sources Analysis in Four Large Cities in China,
761 *Aerosol Air Qual. Res.*, 15, 1836–1843, 2015.
- 762 Li, L., Chen, C. H., Fu, J. S., Huang, C., Streets, D. G., Huang, H. Y., and Fu, J. M.: Air quality and emissions in the Yangtze River
763 Delta, China, *Atmos. Chem. Phys.*, 11(4), 1621–1639, 2011.
- 764 Liu, Y., Li, L., An, J. Y., Zhang, W., Yan, R. S., L. H., and M, W.: Emissions, chemical composition, and spatial and temporal allocation
765 of the BVOCs in the Yangtze River Delta Region in 2014, *Environ. Sci.*, 39(2), 2018.
- 766 Li, M., Zhang, Q., Kurokawa, J.-i., Woo, J.-H., He, K., Lu, Z., and Zheng, B.: MIX: a mosaic Asian anthropogenic emission inventory
767 under the international collaboration framework of the MICS-Asia and HTAP, *Atmos. Chem. Phys.*, 17(2), 935–963, 2017.
- 768 Lin, Y. L.: Bulk parameterization of the snow field in a cloud model, *J. Appl. Meteorol.*, 22(6), 1065–1092, 1983.
- 769 Li, L., Chen, C. H., Fu, J. S., Huang, C., Streets, D. G., Huang, H. Y., Zhang, G. F., Wang, Y. J., Jang, C. J., Wang, H. L., Chen, Y. R.,
770 and Fu, J. M.: Air quality and emissions in the Yangtze River Delta, China, *Atmos. Chem. Phys.*, 11, 1621–1639, 2011.
- 771 Li, L., An, J. Y., Zhou, M., Yan, R. S., Huang, C., Lu, Q., Lin, L., Wang, Y. J., Tao, S. K., Qiao, L. P., Zhu, S. H., and Chen, C. H.:
772 Source apportionment of fine particles and its chemical components over the Yangtze River Delta, China during a heavy haze
773 pollution episode, *Atmos. Environ.*, 123, 415–429, 2015.
- 774 Li, M., Zhang, Q., Kurokawa, J.-i., Woo, J.-H., He, K., Lu, Z., Ohara, T., Song, Y., Streets, D. G., Carmichael, G. R., Cheng, Y., Hong,
775 C., Huo, H., Jiang, X., Kang, S., Liu, F., Su, H., and Zheng, B.: MIX: a mosaic Asian anthropogenic emission inventory under the
776 international collaboration framework of the MICS-Asia and HTAP, China, *Atmos. Chem. Phys.*, 17, 935–963, 2017.
- 777 Li, X., Zhang, Q., Zhang, Y., Zheng, B., Wang, K., Chen, Y., Wallington, T. J., Han, W., Shen, W., Zhang, X., and He, K.: Source
778 contributions of urban PM 2.5 in the Beijing–Tianjin–Hebei region: Changes between 2006 and 2013 and relative impacts of
779 emissions and meteorology, *Atmos. Environ.*, 123, 229–239, 2015.
- 780 Lin, Y. L.: Bulk parameterization of the snow field in a cloud model, *J. Appl. Meteorol.*, 22, 1065–1092, 1983.
- 781 Liu, Y., Li, L., An, J. Y., Zhang, W., Yan, R. S., L. H., Huang, C., Wang, H. L., Q, W., and M, W.: Emissions, chemical composition,
782 and spatial and temporal allocation of the BVOCs in the Yangtze River Delta Region in 2014, *Environ. Sci.*, 39, 608–617, 2018.
- 783 Liang, P. F., Zhu, T., Fang, Y. H., Li, Y. R., Han, Y. Q., Wu, Y. S., Hu, M., and Wang, J. X.: The role of meteorological conditions



- 784 and pollution control strategies in reducing air pollution in Beijing during APEC 2014 and Victory Parade 2015, *Atmos. Chem.*
785 *Phys.*, 17, 13921–13940, 2017.
- 786 Liu, J., and Zhu, T.: NOx in Chinese Megacities, *Nato. Sci. Peace. Secur.*, 120, 249–263, 2013.
- 787 Markovic, M. Z., VandenBoer, T.C., and Murphy, J. G.: Characterization and Optimization of an Online System for the Simultaneous
788 Measurement of Atmospheric Water-soluble Constituents in the Gas and Particle Phases, *J. Environ. Monit.*, 14, 1872–1874, 2012.
- 789 Mlawer, E. J., Taubman, S. J., Brown, P. D., Iacono, M. J., and Clough, S. A.: Radiative transfer for inhomogeneous atmospheres:
790 RRTM, a validated correlated-k model for the longwave, *J. Geophys. Res.*, 102(D14), 16663-16682, 1997.
- 791 Nolte, C. G., Appel, K. W., Kelly, J. T., Bhawe, P. V., Fahey, K. M., Collet Jr., J. L., Zhang, L., and Young, J. O.: Evaluation of the
792 Community Multiscale Air Quality (CMAQ) model v5.0 against size-resolved measurements of inorganic particle composition
793 across sites in North America, *Geosci. Model Dev.*, 8, 2877-2892, 2015.
- 794 Nenes, A., Pilinis, C., and Pandis, S. N.: ISORROPIA: A New Thermodynamic Model for Multiphase Multicomponent Inorganic
795 Aerosols, *Aquat. Geochem.*, 4, 123-152, 1998.
- 796 Pui, D. Y. H., Chen, S. C., and Zuo, Z. L.: PM2.5 in China: Measurements, sources, visibility and health effects, and mitigation,
797 *Particuology*, 13, 1-26, 2014.
- 798 Polissar, A. V., Hopke, P. K., Kaufmann, P. P., Kaufmann, Y., Hall, D., Bodhaine, B., Dutton, E., and Harris J.: The aerosol at Barrow,
799 Alaska: long-term trends and source location, *Atmos. Environ.*, 33(16), 2441-2458, 1999.
- 800 Qi, L., Zhang, Y. F., Ma, Y. H., et al.: Source identification of trace elements in the atmosphere during the second Asian Youth Games
801 in Nanjing, China: Influence of control measures on air quality, *Atmos. Pollut. Res.*, 7 (3), 547-556, 2016.
- 802 Swagata, P., Pramod, K., Sunita, V., et al.: Potential source identification for aerosol concentrations over a site in Northwestern India,
803 *Atmos. Res.*, 169, 65-72, 2016.
- 804 Sun, Y. L., Wang, Z. F., Wild, O., et al.: “APEC Blue”: Secondary Aerosol Reductions from Emission Controls in Beijing, *Sci. Rep.*
805 *UK.*, 6, 20668, 2016.
- 806 Tang, L., Haeger-Eugensson, M., Sjoberg, K., et al.: Estimation of the long-range transport contribution from secondary inorganic
807 components to urban background PM10 concentrations in south-western Sweden during 1986-2010, *Atmos. Environ.*, 89, 93-101,
808 2014.
- 809 Tang, G., Zhu, X., Hu, B. et al.: Impact of emission controls on air quality in Beijing during APEC 2014: lidar ceilometer observations,
810 *Atmos. Chem. Phys.*, 15, 12667–12680, 2015.
- 811 Tian, Mi., Wang, H. B., Chen, Y., et al.: Characteristics of aerosol pollution during heavy haze events in Suzhou, China, *Atmos. Chem.*
812 *Phys.*, 16, 7357–7371, 2016.
- 813 US EPA.: Draft Modeling Guidance for Demonstrating Attainment of Air Quality Goals for Ozone, PM2.5, and Regional Haze, 2014.
- 814 Wang, L. T., Wei, Z., Yang, J., Zhang, Y., Zhang, F. F., Su, J., Meng, C. C., and Zhang, Q.: The 2013 severe haze over southern Hebei,



- 815 China: model evaluation, source apportionment, and policy implications, *Atmos. Chem. Phys.*, 14, 3151-3173, 2014.
- 816 Wang, Y. Q., Zhang, X. Y., and Draxler, R. R.: TrajStat: GIS-based software that uses various trajectory statistical analysis methods
817 to identify potential sources from long-term air pollution measurement data, *Environ. Modell. Softw.*, 24(8), 938-939, 2009.
- 818 West, J. J., Cohen, A., Dentener, F., Brunekreef, B., Zhu, T., Armstrong, B., Bell, M. L., Brauer, M., Carmichael, G., Costa, D. L.,
819 Dockery, D. W., Kleeman, M., Krzyzanowski, M., Künzli, N., Lioussé, C., Lung, S. C., Martin, R. V., Pöschl, U., Pope, C. A.,
820 Roberts, J. M., Russell, A. G., and Wiedinmyer, C.: "What We Breathe Impacts Our Health: Improving Understanding of the Link
821 between Air Pollution and Health", *Environ. Sci. Technol.*, 50 (10), 4895-4904, 2016.
- 822 Wang, T., Nie, W., Gao, J., et al.: Air quality during the 2008 Beijing Olympics: secondary pollutants and regional impact, *Atmos.*
823 *Chem. Phys.*, 10, 7603-7615, 2010.
- 824 Wang, Y., Hao, J., McElroy, M. B., et al.: Ozone air quality during the 2008 Beijing Olympics: effectiveness of emission restrictions,
825 *Atmos. Chem. Phys.*, 9, 5237-5251, 2009.
- 826 Wang, Y. Q., Zhang, Y., Schauer, J. J., et al.: Relative impact of emissions controls and meteorology on air pollution mitigation
827 associated with the Asia-Pacific Economic Cooperation (APEC) conference in Beijing, China, *Sci. Total Environ.*, 571, 1467-1476,
828 2016.
- 829 Wang, Z. S., Li, Y. T., Chen, T., et al.: Changes in atmospheric composition during the 2014 APEC conference in Beijing, *J. Geophys.*
830 *Res.*, 120 (24), 2015.
- 831 Wang, Q. Z., Zhuang, G. S., Huang, Kan., et al.: Probing the severe haze pollution in three typical regions of China: Characteristics,
832 sources and regional impacts, *Atmos. Environ.*, 120, 76-88, 2015.
- 833 Xu, W., Song, Wei., Zhang, Y. Y., et al.: Air quality improvement in a megacity: implications from 2015 Beijing Parade Blue pollution
834 control actions, *Atmos. Chem. Phys.*, 17, 31-46, 2017.
- 835 Xiao, Z. M., Zhang, Y. F., Hong, S. M., et al.: Estimation of the Main Factors Influencing Haze, Based on a Long-term Monitoring
836 Campaign in Hangzhou, China, *Aerosol Air Qual. Res.*, 11, 873-882, 2011.
- 837 Yang, H. N., Chen, J., Wen, J. J., et al.: Composition and sources of PM_{2.5} around the heating periods of 2013 and 2014 in Beijing:
838 Implications for efficient mitigation measures, *Atmos. Environ.*, 124, 378-386, 2016.
- 839 Yu, S. C., Saxena, V. K., Zhao, Z.: A comparison of signals of regional aerosol-induced forcing in eastern China and the southeastern
840 United States, *Geophys. Res. Lett.*, 28, 713-716, 2001.
- 841 Yu, S. C., Zhang, Q. Y., Yan, R. C., et al.: Origin of air pollution during a weekly heavy haze episode in Hangzhou, China, *Environ.*
842 *Chem. Lett.*, 12, 543-550, 2014.
- 843 Yarwood, G., Rao, S., Yocke, M., et al.: Updates to the Carbon Bond chemical mechanism: CB05, Final Report prepared for US EPA,
844 2005.
- 845 Zhang, Y., Cheng, S. H., Chen, Y. S., and Wang, W. X.: Application of MM5 in China: Model evaluation, seasonal variations, and



- 846 sensitivity to horizontal grid resolutions, *Atmos. Environ.*, 45, 3454-3465, 2011.
- 847 Zheng, B., Zhang, Q., Zhang, Y., He, K. B., Wang, K., Zheng, G. J., Duan, F. K., Ma, Y. L., and Kimoto, T.: Heterogeneous chemistry:
848 a mechanism missing in current models to explain secondary inorganic aerosol formation during the January 2013 haze episode in
849 North China, *Atmos. Chem. Phys.*, 15, 2031-2049, 2015.
- 850 Zeng, Y., and Hopke, P. K.: A study of the sources of acid precipitation in Ontario, Canada, *Atmos. Environ.*, 23(7), 1499-1509, 1989.
- 851 Zhang, X. Y., Wang, Y. Q., Niu, T., et al.: Atmospheric aerosol compositions in China: spatial/temporal variability, chemical signature,
852 regional haze distribution and comparisons with global aerosols, *Atmos. Chem. Phys.*, 12, 779-799, 2012.
- 853 Zhang, Y. J., Tang, L. L., Wang, Z., et al.: Insights into characteristics, sources, and evolution of submicron aerosols during harvest
854 seasons in the Yangtze River delta region, China, *Atmos. Chem. Phys.*, 15, 1331-1349, 2015.